Australian Government
Geoscience Australia

Interpretation of Seismic Data, Capel and Faust Basins, Australia's Remote Offshore Eastern Frontier

J. B. Colwell, T. Hashimoto, N. Rollet, K. Higgins, G. Bernardel and S. McGiveron

Record
2010/06

GeoCat #
69190

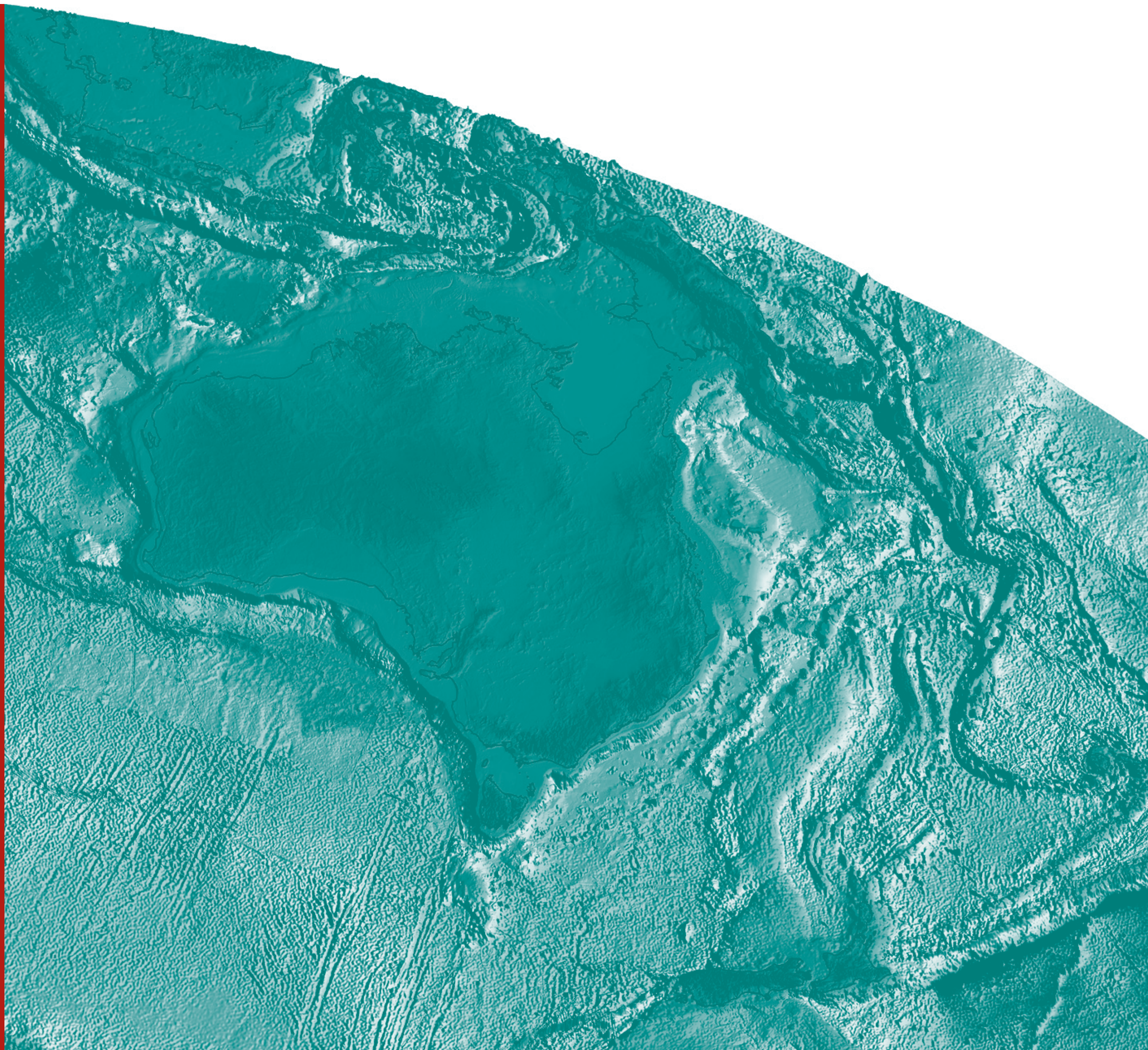

Interpretation of Seismic Data, Capel and Faust Basins, Australia's Remote Offshore Eastern Frontier

GEOSCIENCE AUSTRALIA
RECORD 2010/06

by

J. B. Colwell*, T. Hashimoto, N. Rollet, K. Higgins, G. Bernardel and S. McGiveron**

Australian Government
Geoscience Australia

RPS

* formerly Geoscience Australia
** RPS Energy

Department of Resources, Energy and Tourism
Minister for Resources and Energy: The Hon. Martin Ferguson, AM MP
Secretary: Mr Drew Clark

Geoscience Australia
Chief Executive Officer: Dr Chris Pigram

ISSN 1448-2177
ISBN 978-1-921672-63-7

GeoCat Number 69190

Bibliographic reference: Colwell, J. B., Hashimoto, T., Rollet, N., Higgins, K., Bernardel, G. and McGiveron, S., 2010. Interpretation of Seismic Data, Capel and Faust Basins, Australia's Remote Offshore Eastern Frontier. Geoscience Australia Record 2010/06.

Contents

FIGURES

CF_Olig (pink) horizon. A description of probable mud volcanoes at about the CF_Olig (pink) horizon is given in Appendix 2. See Table 1 for identification of the coloured horizons and Figure 19 for the location of the examples.

Figure 21. Map showing the thickness of the Post-rift Megasequence in milliseconds TWT. The map is generated from the seismic horizons CF_Sr2B and CF_Wb (see Table 1).

Figure 22. Example of a possible diagenetic bottom simulating reflector (BSR) within the Upper Sag section of the Post-rift Megasequence seen in the seismic data. Location of the example is shown in Figure 21.

Figure 23. Examples of structuring within the Syn-rift 1 Megasequence seen in the seismic data. Note the prominent 'pop-up' structure composed of Syn-rift 1 sediments at the centre of (a). See Table 1 for identification of the coloured horizons and Figure 24 for the location of the examples.

Figure 24. Location of the examples shown in Figures 23 and 27. Base map is the Syn-Rift 1 time isopach map (Figure 14).

Figure 25. Examples of the structuring within the Syn-rift 2 Megasequence seen in the seismic data. Note the prominent 'pop-up' structure composed of Syn-rift 2 sediments at the centre of (a) and associated folding and onlap of the overlying Post-rift Megasequence. See Table 1 for identification of the coloured horizons and Figure 26 for the location of the examples.

Figure 26. Location of the examples shown in Figure 25. Base map is the Syn-rift 2 time isopach map (Figure 17).

Figure 27. Example of basin inversion and fault reactivation seen in the seismic data. See Table 1 for identification of the coloured horizons and Figure 28 for the location of the example. Continued movement on the main fault (centre right) has produced a seafloor scarp, followed by current erosion and/or non-deposition on the face of the scarp. These types of seafloor features are well imaged on the GA survey 2436 (TAN031) swath bathymetry data (see Heap et al., 2009).

Figure 28. Location of the example shown in Figure 27. Base map is the total sediment thickness above basement in milliseconds TWT (Figure 12).

TABLES

APPENDICES

Executive Summary

The Capel and Faust basins are located in a remote part of deepwater offshore eastern Australia. They encompass a series of Cretaceous rift depocentres within the northern part of the Lord Howe Rise, a continental fragment that became detached from Australia during the breakup of the eastern Gondwana and the opening of the Tasman Sea Basin.

As part of Geoscience Australia (GA)'s ongoing work to identify and evaluate the petroleum potential of Australia's offshore frontier basins, approximately 6000 km of industry-standard, 106-fold 2D seismic data were acquired over the Capel and Faust basins during late 2006 and early 2007. These data significantly improved the previously very sparse regional data coverage. In addition to the seismic data, GA acquired approximately 24,000 km^2 of multibeam bathymetry and 11,000 line km of shipboard gravity and magnetic data.

This GA Record details the results of interpretation of the seismic data and is intended to complement the release of a digital version of the interpretations. Additional conclusions drawn from the seismic interpretations and the integrated analysis of the seismic, potential field and other data sets currently being completed at GA are beyond the scope of this record. These results have been, or will be, published in other GA Records, peer-reviewed journals and conference proceedings.

The seismic data has confirmed the presence of multiple depocentres in the Capel and Faust basins. The largest depocentres are located in the northwestern and central parts of the seismic grid, where the combined ?Cretaceous and Cenozoic successions attain 3.6 seconds two-way time (TWT) or about 6.2 km. Twelve seismic horizons and two fault types have been interpreted throughout the grid. The major seismic horizons delineate three pre-rift basement facies and megasequence boundaries of two syn-rift and one post-rift successions:

- 'Layered' basement of probable Mesozoic sedimentary origin including coal measures;
- 'Bland' basement possibly comprising heterogenous and/or highly structured rocks including metamorphics and intrusive rocks;
- 'Volcanic' basement of pre-rift to earliest syn-rift (?Early Cretaceous) volcanic and intrusive rocks;
- Syn-rift 1 Megasequence dominated by ?Early Cretaceous–?Cenomanian non-marine and volcaniclastic sediments, volcanics and intrusives up to 2.2 seconds TWT thick;
- Syn-rift 2 Megasequence dominated by ?Cenomanian–?Campanian non-marine to marginal marine siliciclastic sediments thicknening westward to a maximum thickness of 1.4 seconds TWT;
- Post-rift Megasequence of ?Campanian to Recent predominantly bathyal sediments up to 1.8 seconds TWT thick. DSDP hole 208, located in the far northern part of the seismic grid, provides age and lithological control for the upper (predominantly Cenozoic) part of this megasequence.

The region is structurally complex. Seismic interpretation and potential field data (particularly the Bouguer gravity) reveal a series of compartmentalised fault-bounded depocentres (graben and half-graben) and, to a lesser extent, sag depocentres. The largest depocentres are up to 120 km long and 40 km wide. The largest basin-bounding, basement-offsetting and intra-basin faults were interpreted throughout the seismic grid. Widepsread small Cenozoic faults, many of which are polygonal faults, were not interpreted. Major faults were formed throughout the study area during the Syn-rift 1 phase, but major faulting during the Syn-rift 2 phase was restricted to the western areas. This apparent shift in the locus of extension probably represents the lead up to the opening of the Tasman Sea.

Significant deformation and uplift events occur at the end of, or following, the two syn-rift phases and during the post-rift phase. Several of the major depocentres show evidence of probable transpression that have resulted in uplift and erosion of structural highs, gentle folding of basin sediments, fault reactivation and localised inversion on some faults.

The seismic interpretation presented in this GA Record contributes to the integrated assessment of the Capel and Faust basins being completed at GA, and provides significantly improved geoscientific and prospectivity information on this under-explored frontier region. The results indicate that sediments within the basins are sufficiently thick for petroleum generation, which has also been confirmed by 1D basin modelling (Hashimoto et al., 2010). Regional correlations suggest that potential petroleum source, reservoir and seal rocks are likely to be present. Future additional data acquisition in the region through stratigraphic drilling and targeted seismic surveys would greatly reduce the uncertainties associated with the current interpretations.

Introduction

The Capel and Faust basins are located in the northern Tasman Sea, offshore eastern Australia, in water depths of approximately 1300–2500m (Figure 1). This record details an interpretation of seismic data from these basins undertaken by Geoscience Australia (GA)'s Remote Eastern Frontiers Project in 2008 and the early part of 2009. The interpretation focused on the 6023 km of 2D seismic reflection data acquired by GA as part of survey GA-302 during November 2006 to January 2007. It also included three reprocessed line segments from GA's 1998 regional seismic survey GA-206 (lines GA-206r/04 and 206r/02a and b; totalling approximately 650 km; Figures 2 and 3). The data acquisition and interpretation form part of GA's ongoing work to identify offshore frontier basins within Australia's marine jurisdiction, to provide pre-competitive geoscientific information to industry, and to high-grade petroleum prospectivity of Australia's remote frontier areas. Funding for this work is provided to GA by the Australian Government under the Energy Security Program (2006–2011).

Initial interpretation of the GA-302 seismic data has provided input into a number of papers and abstracts, e.g. Hashimoto et al. (2008a, b, c), Norvick et al. (2008), Petkovic et al. (2008, 2010) and Hackney et al. (2009a, b, 2010). Earlier interpretations of sparse regional seismic lines acquired during the 1970s to 1990s are summarised in Van de Beuque et al. (2003). The work described in this record provides an important input to understanding the geology and hydrocarbon potential of the region. Critical to this understanding is the integration of seismic, potential field and other data sets, including geohistory modelling. This record details the seismic interpretation component of the data integration and provides background information to accompany the release of a digital seismic interpretation project in GeoFrame™ and other workstation formats. Details of the seismic tie to DSDP hole 208 and an analysis of seismic features in the upper part of the sedimentary succession are included in Appendices 1 and 2 respectively, and pdf files of interpreted and un-interpreted versions of the seismic lines are included in Appendix 3.

Other GA records published by the Remote Eastern Frontiers Project address aspects of the potential field (gravity and magnetic) data sets (Hackney, 2010), velocity and potential field modelling (Petkovic, 2010; Petkovic et al., in prep.), and 3D geological modelling (Higgins et al., in prep.). The scientific conclusions drawn from the integration of the different data sets are presented in a series of scientific journal and conference papers.

REGIONAL SETTING

The Capel and Faust basins are Cretaceous rifts within the Lord Howe Rise, a continental fragment that extends approximately 1600 km from southwest of New Caledonia to the Bellona Trough (Figure 1). The area is located near the former eastern Gondwana plate margin, a locus of convergent tectonics throughout much of the Palaeozoic and Mesozoic (Gaina et al., 1998; Veevers, 2000; Sdrolias et al., 2001; Crawford et al., 2003; Schellart et al., 2006). Extension took place in the back arc region of the margin from the Early Cretaceous, culminating with the opening of the Tasman Sea (Hayes and Ringis, 1973; Gaina et al., 1998; Sdrolias et al., 2001; Crawford et al., 2003). This produced the current structural configuration of the region, which features a mosaic of continental fragments, rifts and small oceanic basins (Gaina et al., 1998; Sdrolias et al., 2001; Norvick et al., 2001, 2008). The Lord Howe Rise is the largest of the continental fragments with an estimated crustal thickness of 14–34 km (Shor et al., 1971; Zhu and Symonds, 1994). The rifting of the Lord

Howe Rise from eastern Australia was strongly asymmetric. Jongsma and Mutter (1978) and Etheridge et al., (1989) conceptualised the Lord Howe Rise as the 'lower plate margin' of a simple shear model, composed of extended continental crust. The rise is flanked to the east and west by basins that predominantly exhibit sag geometries (e.g. Middleton, Fairway and New Caledonia; Auzende et al. 2000a; Lafoy et al. 2005; Exon et al. 2007; Norvick et al., 2008) and smaller continental fragments (e.g. Dampier Ridge; McDougall et al., 1994). Some of the sag basins may be underlain by transitional or oceanic crust (Shor et al., 1971; Gaina et al., 1998; Lafoy et al., 2005; Norvick et al., 2008).

The Lord Howe Rise exhibits a N–S to NW–SE structural trend and may be subdivided into three major structural zones (Stagg et al., 1999, 2002; Willcox et al., 2001; Van de Beuque et al., 2003). The Lord Howe Platform (Stagg et al., 1999, 2002; Van de Beuque et al., 2003; Figure 1) is an eastern zone of high-standing basement, 100–200 km wide and in water depths of 1000–1300 m. Crustal thicknesses of 29–34 km (Shor et al., 1971; Zhu and Symonds, 1994) and the limited development of rift depocentres indicate that little crustal thinning took place here during the rifting (Van de Beuque et al., 2003). It is mantled by a thin (0–0.5 s TWT) cover of mostly Cenozoic bathyal sediments.

The Central Rift Province (Stagg et al, 1999, 2002; Van de Beuque et al., 2003) lies to the west of the Lord Howe Platform in water depths of 1300–1700 m (Figures 1 and 4). It includes the Faust Basin in the northern Lord Howe Rise and the Moore Basin to the south. It comprises a series of basement highs and comparatively small, rift depocentres with sediment thicknesses of 1–2 s TWT. The sedimentary succession within the depocentres is likely to be dominated by Lower and Upper Cretaceous syn-rift clastics and volcanics, which are overlain by a Campanian to Recent sag sequence grading upward from non-marine or marginal marine clastics to bathyal carbonates (Willcox and Sayers, 2002; Van de Beuque et al., 2003; Norvick et al., 2008).

The rift depocentres are larger and deeper further westward in the Western Rift Province (Stagg et al., 1999, 2002; Van de Beuque et al., 2003), which includes the Capel Basin in the north and the Monowai Basin in the south (Figures 1 and 4). In the central part of the Lord Howe Rise, the Central and Western Rifts merge to form the Gower Basin (Stagg et al., 1999; Willcox and Sayers, 2002; Colwell et al., 2006). Individual depocentres are up to 150 km long and 40 km across and are filled with sediments 2–3 s TWT thick. This general westward increase in the degree of rift development reflects increased crustal thinning from the Lord Howe Platform through to the Middleton Basin. Crustal thicknesses in the Central and Western Rift Provinces are estimated to be less than 20 km (Shor et al., 1971; Zhu and Symonds, 1994).

Evidence for Cenozoic post-rift igneous activity is widespread throughout the Lord Howe Rise region. The most prominent are the Tasmantid and Lord Howe seamount chains to the east of the Lord Howe Rise (Slater and Goodwin, 1973; McDougall et al., 1981). Numerous smaller volcanic features occur away from the seamount chains. Some are exposed at the seafloor, such as the early Miocene examples described by Exon et al. (2004), but many others are concealed by bathyal sediments and are only apparent in seismic data.

The Deep Sea Drilling Program (DSDP) hole 208 (Figures 2 and 3) provides the only well control in the Capel and Faust basins. The drill hole intersected 594 m of post-rift nannofossil chalk and ooze of Late Maastrichtian to Recent age (The Shipboard Party, 1973c; Andrews, 1973). Four core holes comprising the DSDP 588 site, with a maximum depth of 488 m below the sea bed, were drilled at the same location in 1982. There are no petroleum exploration wells in the area. The syn-rift and pre-rift successions have not been drilled.

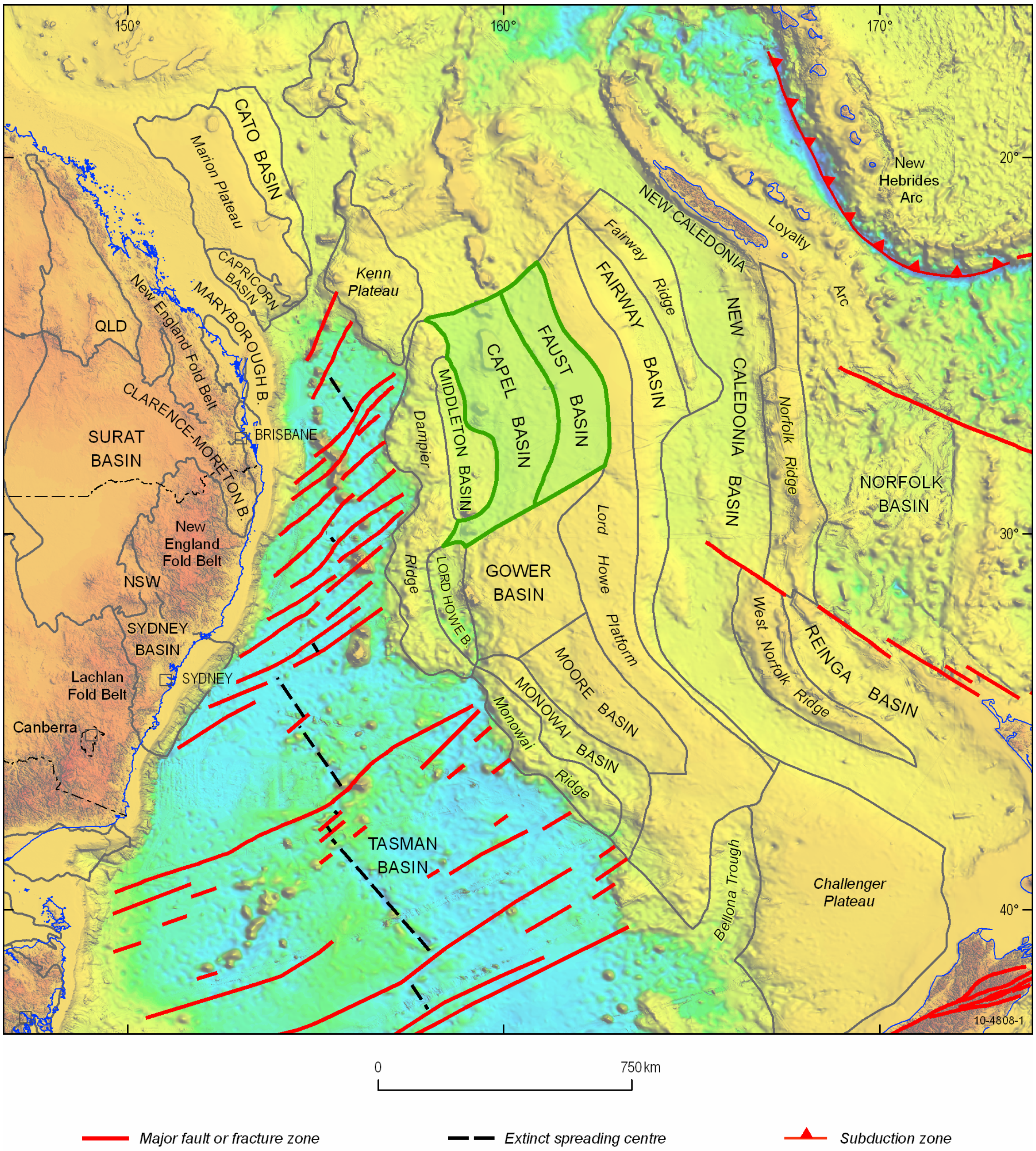

Figure 1: *Regional setting of the Capel and Faust basins.*

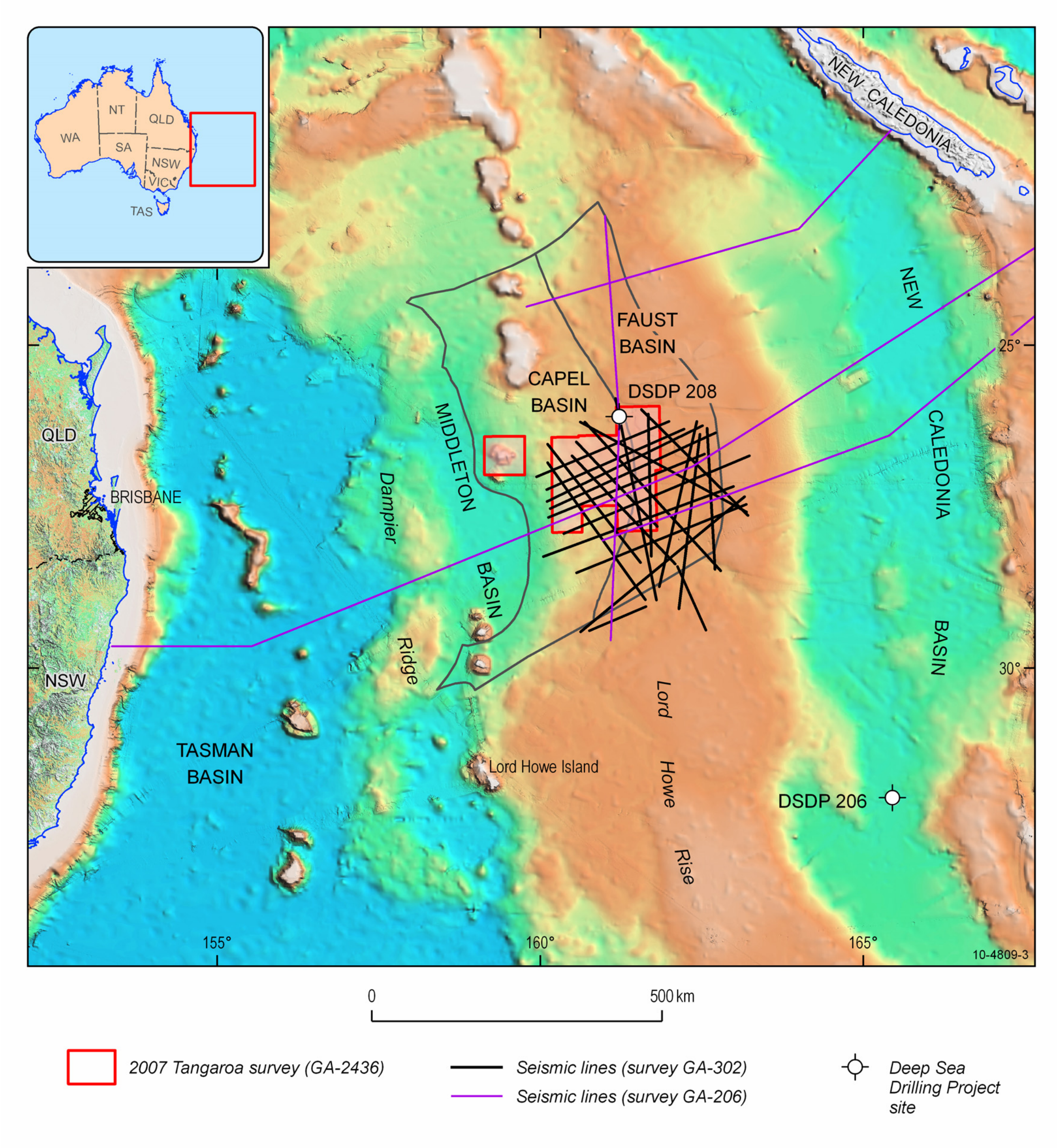

Figure 2: *Location of the GA-206, GA-302 and GA-2436 surveys over the Lord Howe Rise.*

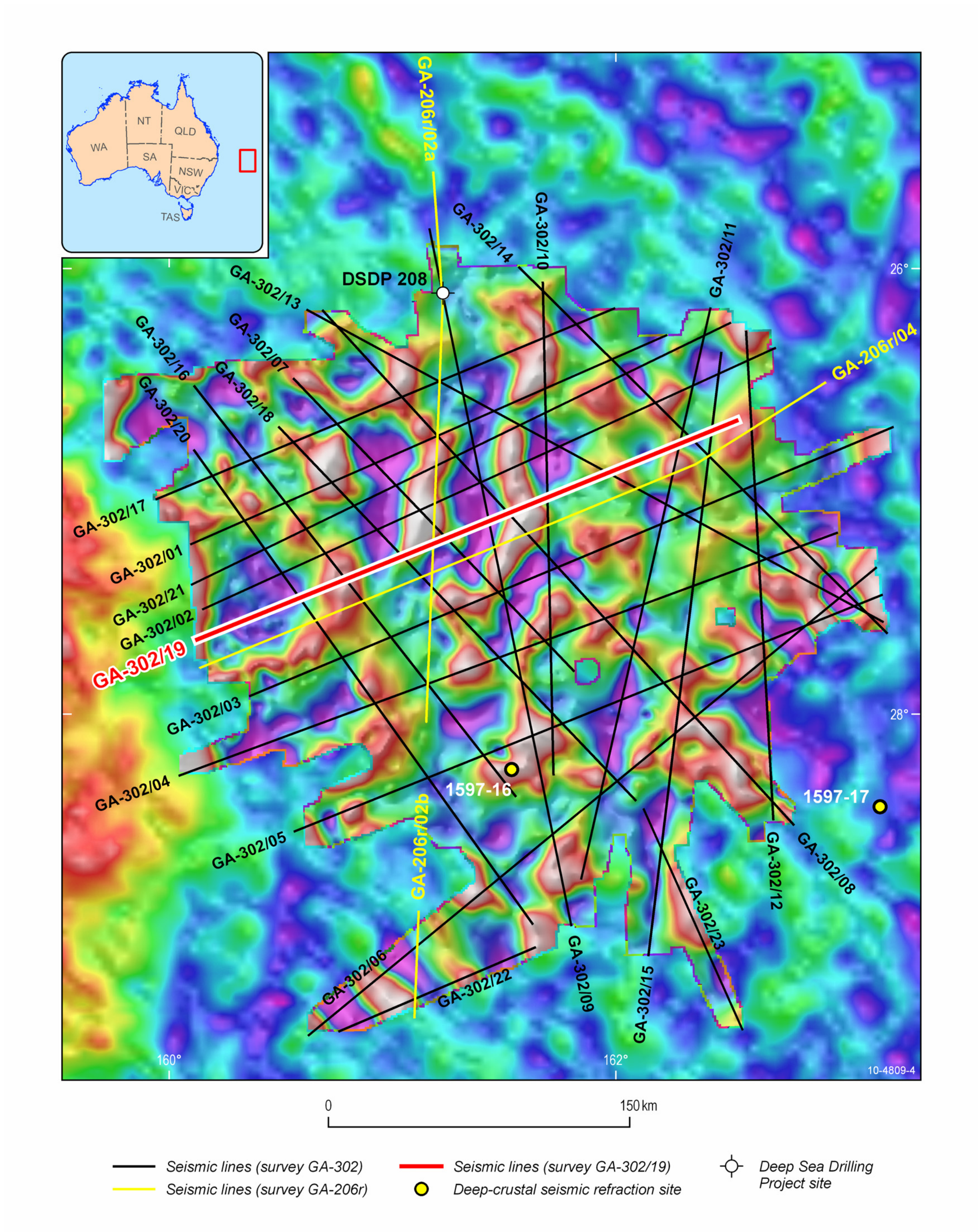

Figure 3: *Location of GA-206 and GA-302 seismic lines interpreted as part of the present study. The line locations are superimposed on an image of bandpass-filtered Bouguer gravity (see Hackney, 2010). The gravity image is a composite of shipboard gravity for the grid area superimposed on satellite altimeter-derived gravity for the areas beyond the grid. The location of two deep-crustal seismic refraction experiments (1597-16 and 1597-17; Shor et al., 1971) are also shown.*

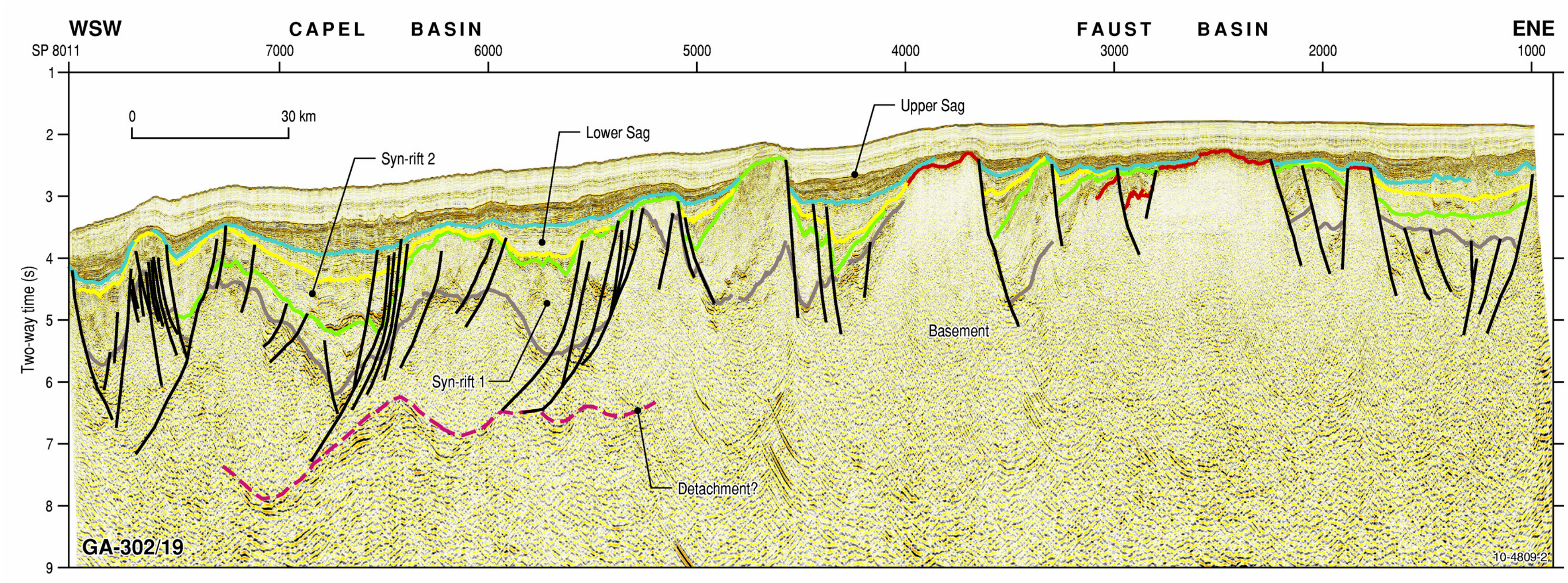

Figure 4: *Seismic line GA-302/19 showing the general rift architecture of the northern Lord Howe Rise across the Capel and Faust basins. Location of the seismic line is shown in [Figure 3](#).*

PREVIOUS WORK

Pre-2000 work on the northern Lord Howe Rise is summarised by Van de Beuque et al. (2003). Similar syntheses for the central and southern Lord Howe Rise are presented by Willcox & Sayers (2002) and Stagg et al. (2002) respectively. All these reports were prepared by the Law of the Sea Project (1998–2004) at GA as part of Australia's 2004 submission to the United Nations (UN) for areas of extended continental shelf as defined by Article 76 of the UN Convention on the Law of the Sea (UNCLOS).

Previous marine surveys in the Capel and Faust basins have acquired seismic, bathymetry, gravity, magnetic and geological sample data sets. The German–Australian RV *Sonne* 36A survey in 1985 mostly acquired seismic data in the Gower Basin to the south of the Capel and Faust basins, but also collected dredge samples of continental rocks from the Lord Howe Platform to the southeast of the GA-302 seismic grid (Roser et al., 1985). The GA-206 survey in 1998 was completed as part of a French–Australian co-operative study (FAUST 1), and acquired 4564 km of high-quality seismic data from the eastern Australian continental margin to southeast of New Caledonia including the Capel and Faust basins (Figure 2). In 2006, GA acquired cores of Cenozoic sediments, rock dredge samples, heatflow measurements and bathymetry, gravity and magnetic data from the Capel, Faust, Fairway and New Caledonia basins and the surrounding areas during the French–Australian AUSFAIR survey (RV *Marion Dufresne*; Colwell et al., 2006). Dredging during this survey recovered volcanic and shallow marine rock samples of Cretaceous age (Colwell et al., 2006; Higgins et al., in press).

DATA ACQUISITION AND PROCESSING

Seismic survey GA-302 (Figure 2) was shot by the CGG-operated seismic vessel MV *Pacific Titan* from 19 November 2006 to 7 January 2007. The survey area is located within the Australian EEZ and extended continental shelf to the south of the Australia–France 1982 treaty boundary (Figure 2). 6023 km of seismic data were acquired on 23 lines with a spacing generally ranging from 20 to 50 km (Figure 3). The placement of the GA-302 lines was significantly guided by filtered satellite altimeter-derived gravity data (Sandwell and Smith, 1997). An inspection of the gravity data in conjunction with the GA-206 and other pre-existing seismic data suggested that the location of basin depocentres along the seismic lines generally correlated with areas of gravity lows (Kroh et al., 2007). The GA-302 grid was designed to optimise the alignment of the seismic lines with the axes of the major gravity lows, and thus to maximise the likelihood of imaging the largest depocentres in the area.

The GA-302 seismic data were collected as 12 second TWT records using an 8 km long solid streamer configured with a 12.5 m group spacing producing 106-fold coverage from a shot interval of 37.5 m. Gravity, magnetic, bathymetry and long-offset reflection and refraction (sonobuoy) data were also acquired during the survey (Kroh et al., 2007). The magnetic, gravity and bathymetry data were subsequently processed by Fugro Robertson Inc.

After collection, the following standard processing sequence was applied to the GA-302 seismic data by Fugro Seismic Imaging Pty Ltd:

- Swell Noise Attenuation
- Radon in the Shot domain targeting WB multiple
- Linear Tau-P mute to preserve long offset information

- Surface Related Multiple Elimination (SRME) with cascaded adaptive subtraction
- High Resolution Radon Demultiple (CMP domain)
- Curved Ray Anisotropic Kirchhoff Pre Stack Time Migration (PreSTM)
- 4th Order NMO and Eta corrections using 3rd pass velocities
- Statistically derived minimum to zero phase conversion
- Near, Middle and Far angle stacks
- CMP gathers with and without 4th Order NMO and Eta corrections

For survey GA-302, the following data types are available from GA (contact: ausgeodata@ga.gov.au) at the cost of transfer:

- Full PreSTM stacks
- Full PreSTM stacks with Dual Gate AGC Scalars
- Full PreSTM stacks with Dual Gate AGC Scalars and Inverse Q
- Near, Middle and Far angle stacks
- Near, Middle and Far angle stacks with Inverse Q
- PreSTM CMP gathers on 3592 tapes
- PreSTM CMP gathers with 4th order NMO and Eta corrections on 3592 tapes
- Velocities, Navigation and Observer logs
- Processed Magnetic and Gravity data
- Field Data on 3592 tapes

Seismic data from the GA-206 survey (also known as FAUST 1; Figure 2), acquired by RV *Rig Seismic* in 1998, were used to supplement the GA-302 data in this study. A 3–4 km long streamer was used to record data to 16 seconds TWT, at a 12.5 m group interval and a 50 m shot interval producing 30–40-fold seismic coverage (Lafoy et al., 1998b; Bernardel et al., 1999; Van de Beuque et al., 2003). Gravity and magnetic data were also acquired. The seismic data were first processed in 1999 and selected parts of the survey were re-processed in 2006. Details of the processing sequences are available from GA (contact: ausgeodata@ga.gov.au). The GA-206 survey area straddles both Australian and French marine jurisdictions (Figure 2), but the interpretation of the GA-206 data in this study was confined to three reprocessed line segments from the Australian part of the Capel and Faust basins (Figure 3).

In addition, data from the GA-2436 (TAN0713) survey (Figure 2), completed in late 2007 using the New Zealand vessel RV *Tangaroa*, were used to supplement the interpretation of seismic data in this study. The survey, which aimed to improve the geophysical data coverage over the large depocentres in the central part of the Capel and Faust basins, acquired approximately 24,000 km^2 of multibeam bathymetry and 11,000 line km of gravity and magnetic data with a line spacing of 3–4 km (Heap et al., 2009).

Methodology

The seismic lines were interpreted digitally using the Schlumberger GeoFrame™ software. The work was first focused in the northwestern part of the GA-302 seismic grid where the largest and deepest depocentres are located. The interpretation was then progressively extended to the east and south, concentrating on the major depocentres.

The digital interpretations follow earlier 'on-paper' interpretations of parts of the grid (e.g. Norvick et al., 2008) and the results of previous workers who had identified a number of regional unconformities in the GA-206 and earlier seismic data (for example, Willcox et al., 2001; Van de Beuque et al., 2003).

A number of major unconformities were also identified by the current study, corresponding to significant structuring events (typically faulting, uplift, inversion and erosion) and bounding the major seismic packages (megasequences). As suggested by previous work, these can be tentatively correlated, in the absence of age control, with major regional tectonic events such as those in the Cenomanian (~100–95 Ma) and Santonian–Campanian (~85–80 Ma) (Veevers, 2000; Norvick et al., 2001, 2008; Willcox et al., 2001; Schellart et al., 2006).

Twelve seismic horizons were mapped in the Capel-Faust seismic dataset and are described in the next chapter. Only the upper four (Cenozoic and seabed) horizons have age control from the DSDP 208 drill hole (The Shipboard Scientific Party, 1973c). The details of the tie between the seismic data and this DSDP hole are given in Appendix 1. In addition to the seismic horizons, major basin-bounding, basement-offsetting and intra-basin faults were identified and mapped.

3D visualisation was used to assist in understanding the stratigraphic and structural relationships between seismic lines, as well as for evaluating the degree of correlation between potential field (gravity and magnetic) and seismic data. In particular, the gridded gravity data (Petkovic et al., 2008; Hackney et al., 2009a, b; Hackney 2010) provided a valuable guide to the interpolation of major structural boundaries between seismic lines. The results of 3D visualisation and geological modelling are described in Higgins et al., in prep.

CHALLENGES

A number of challenges are apparent in interpreting the regional seismic data from the Capel and Faust basins. These are:

<u>(1) The structural complexity of the basins</u> arising from the occurrence of a large number of compartmentalised ?Cretaceous rift depocentres. As a consequence, rapid changes in structure, stratigraphy and sediment thicknesses are observed along, and between, individual seismic lines, making correlation between the lines difficult. In many areas, multiple phases of extension, structuring and erosion are apparent. There is also evidence for lateral movement along accommodation or transfer zones, which has juxtaposed blocks with markedly different seismic characteristics.

<u>(2) The total lack of age and lithological control on the pre-rift, syn-rift and much of the post-rift sedimentary section</u> The only drilling in the Capel-Faust region is at DSDP sites 208 and 588 (both

at the same site), with a maximum penetration of 594 m below seafloor into bathyal nannofossil chalk of late Maastrichtian age (The Shipboard Scientific Party, 1973c; Andrews, 1973). A number of additional samples have been recovered from the area during marine sampling surveys, including: coring of Cenozoic sediments during the AUSFAIR survey (Colwell et al., 2006) and the GA-2436 survey (Heap et al., 2009); rock dredging of a seafloor exposure of continental rocks on the Lord Howe Platform to the southeast of the GA-302 seismic grid during the RV *Sonne* survey in 1985 and by the AUSFAIR survey (Roser et al., 1985; Colwell et al., 2006), and; dredging of Cenozoic volcanic rocks exposed at the seafloor during the GA-2436 survey (Heap et al., 2009).

(3) The widespread presence of apparent igneous rocks including flows, sills and dykes. These are of various ages and in many cases are associated with faults and other lines of weakness within the crust. They commonly mask or 'filter' the underlying seismic signal. In many places it is impossible to distinguish what may be pre-rift igneous basement from early syn-rift volcanics.

(4) The low lateral and vertical continuity of seismic facies within the sedimentary succession. This probably reflects input in a non-marine environment of detritus from a variety of local and distal sources including volcanoes. Many of the depocentres were flanked by high-standing blocks of pre-rift crust until the early Neogene when the blocks, which would have formed a series of mountains and then islands, finally subsided below wave base. The great variability in seismic character (both laterally and vertically) makes the correlation of seismic packages between the depocentres very difficult or impossible, other than at the regional megasequence level. In many depocentres there are numerous local unconformities which, without age control, cannot be correlated with any certainty outside the depocentre. Indeed, in many cases, these local unconformities are probably the products of local structuring (notably inversion) and/or changes in the sediment supply.

(5) The over-migration of some of the deep seismic data and the inability of the processing stream to fully deal with inter-bed multiples and other 'ringing'. These problems stem from the difficulty of processing seismic data (particularly in deriving reliable stacking velocities) in an area that is structurally complex, has rapid lateral and vertical variations in seismic facies, and contains a significant igneous component. The quality of the seismic data may be enhanced in the future using techniques such as pre-stack depth migration.

Seismic Horizons

Twelve horizons and two fault types were interpreted in the seismic grid over the Capel and Faust basins (Table 1). It should be noted, however, that a given horizon may not be represented in some parts of the seismic grid.

Table 1. Details of the interpreted seismic horizons and faults.

Horizons

Designation	*Description*	*GeoFrame™ colour, number, line style*
CF_Wb	Water bottom (sea floor). **Top of Post-rift Megasequence**.	Dark blue, 30, solid
CF_Olig	**Middle Mid-Eocene–Late Oligocene unconformity** in DSDP 208 (Appendix 1; The Shipboard Scientific Party, 1973c). Broadly conformable. Marks a significant change in seismic character from parallel, high-frequency, low-amplitude reflectors above to parallel, high-frequency and amplitude reflectors below	Pink, 3, solid
CF_Eoc	**Middle Paleocene–Middle Eocene unconformity** in DSDP 208 (Appendix 1; The Shipboard Scientific Party, 1973c).	Purple, 35, solid
CF_Usag	**Top of Lower Sag seismic package** (base of Upper Sag package) within the Post-rift Megasequence. Immediately below the Late Maastrichtian TD in DSDP 208.	Blue, 25, solid
CF_Sr2B	**Top of Syn-rift 2 Megasequence (**base of Post-rift Megasequence). Possibly Campanian in age. Generally an erosional unconformity. In depocentres in the NW part of the study area, faults within the underlying Syn-rift 2 Megasequence do not offset the overlying strata. In areas away from the NW area, the horizon commonly marks the top of a sag section rather than top of a section displaying clear syn-rift geometries.	Yellow, 9, solid
CF_Sr2A	**Top of Syn-rift 2A seismic package** within the Syn-rift 2 Megasequence. Restricted in distribution.	Dark blue, 30, solid
CF_Sr1B	**Top of Syn-rift 1 Megasequence** (base of Syn-rift 2 Megasequence). Possibly Cenomanian in age. Major erosional surface. Represents a major structuring event including reactivation/inversion in some depocentres.	Light green, 15, solid
CF_Sr1A	**Top of Syn-rift 1A seismic package** within the Syn-rift 1 Megasequence. Restricted in distribution.	Light tan/grey, 36, solid
CF_Bmtv **CF_Bmtv_up**	**Top of 'volcanic' (volcanic-rich and/or highly intruded) pre-rift basement** or top of early syn-rift volcanics (impossible to distinguish between these two possibilities in most places).	Purple, 35, solid Purple, 35,

uncertain pick		dotted
CF_Bmtl **CF_Bmtl_up** *uncertain pick*	**Top of 'layered' pre-rift basement** or, possibly, top of an early syn-rift sedimentary section (impossible to distinguish between these two possibilities in places because of line spacing and line orientation).	Grey, 24, solid Grey, 24, dotted
CF_Bmtb **CF_Bmtb_up** *uncertain pick*	**Top of 'bland' (seismically opaque or masked) pre-rift basement**. The underlying section contains weak to very weak reflectors in places. Horizon may represent an indurated, planated or eroded 'old' land surface. Commonly exposed as an erosional surface until approximately the Oligocene.	Red, 4, solid Red, 4, dotted
CF_CretRift **CF206_CretRift** *Survey GA206*	**Top of pre-rift basement**. Composite horizon generated by combining the horizons marking the tops of the different basement types. It is the base of the ?Cretaceous syn-rift megasequences, or the base of the Post-rift Megasequence where the syn-rift megasequences are missing across the basement highs. It may exclude early syn-rift volcanics and sediments where these cannot be differentiated from the pre-rift basement.	Bluish green, 26, solid

Faults

CF_Flt1	Major basin-bounding and/or basement-offsetting fault.	Black, heavy, solid
CF_Flt2	Major intra-basin fault.	Black, mid line weight, solid

All of the above horizons and faults are included in the digital Capel-Faust seismic interpretation project released by Geoscience Australia to the public in GeoFrame™ and other workstation formats.

Seismic Sequences

The interpretation of the GA-302 and GA-206 seismic data has identified two syn-rift and one post-rift megasequence overlying a heterogeneous pre-rift basement (Tables 2 and 3). The megasequences and the pre-rift basement are bounded by major, regionally significant horizons as detailed in Tables 1 and 2.

Table 2. Relationship between the seismic horizons and seismic megasequences.

Seismic megasequence (seismic package)	*Bounding horizon*	*Intra-megasequence horizons*
	CF_Wb	
Post-rift (Upper Sag)		CF_Olig CF_Eoc
	CF_Usag	
Post-rift (Lower Sag)		
	CF_Sr2B	
Syn-rift 2		CF_Sr2A (top of Sr2A seismic package where identified)
	CF_Sr1B	
Syn-rift 1		CF_Sr1A (top of Sr1A seismic package where identified)
	CF_CretRift (comprising CF_Bmtl, CF_Bmtb and CF_Bmtv)	
Pre-rift		

Table 3. Characteristics and geologic interpretation of the seismic megasequences. The age, lithology and depositional environments are inferred from regional plate tectonic reconstructions and chronostratigraphic correlation (Figure 5), DSDP 208 stratigraphy and comparison of the seismic character with well-constrained basins such as the Gippsland, Taranaki and Northland basins of New Zealand.

Seismic megasequence	*Seismic package*	*Inferred age*	*Seismic character*	*Inferred lithology*	*Inferred depositional environment*
Post-rift	**Upper Sag**	Oligocene–Recent	Parallel, high-frequency, low-amplitude reflectors	Calcareous foraminiferan and nannofossil chalk and ooze	Bathyal
		Late Maastrichtian–Eocene	Parallel, high-frequency and amplitude reflectors	Siliceous and calcareous chalk, marl, chert	Bathyal
	Lower Sag	?Early Campanian–Late Maastrichtian	Parallel, divergent or clinoformal, variable frequency and amplitude reflectors	Siliciclastic to calcareous sandstone, fining upward to mudstone	Coastal plain to neritic, grading upward to bathyal
Syn-rift 2		?Cenomanian–?Campanian	Parallel, divergent or clinoformal, moderate to high-frequency, moderate-frequency and continuity reflectors in major depocentres, weak sub-parallel reflectors elsewhere	Sandstone, siltstone, mudstone, volcanics and intrusives	Fluvio-lacustrine, coastal plain in upper parts
	Syn-rift 2A	?Cenomanian–?Turonian	Subparallel, chaotic or 'blocky' (rare), high-amplitude and low-continuity reflectors	Volcanics and intrusives, possible coal	Volcanogenic, possible fluvio-lacustrine
Syn-rift 1		?Early Cretaceous–?Cenomanian	Chaotic to layered, variable amplitude and frequency, low-continuity reflectors	Sandstone, siltstone, conglomerate, volcanics and intrusives	Fluvial, colluvial, volcanogenic
	Syn-rift 1A	?Early Cretaceous	Parallel, divergent or 'blocky', high-amplitude, low-frequency, moderate-continuity reflectors	Coal, sandstone, siltstone, volcanics and intrusives	Fluvio-lacustrine, volcanogenic
Pre-rift		?Palaeozoic–Mesozoic	Variable	Various sedimentary (including coal), volcanic, intrusive and metamorphic rocks	E. Cretaceous pre-rift volcanics, Mesozoic sedimentary basins, Palaeozoic fold belt

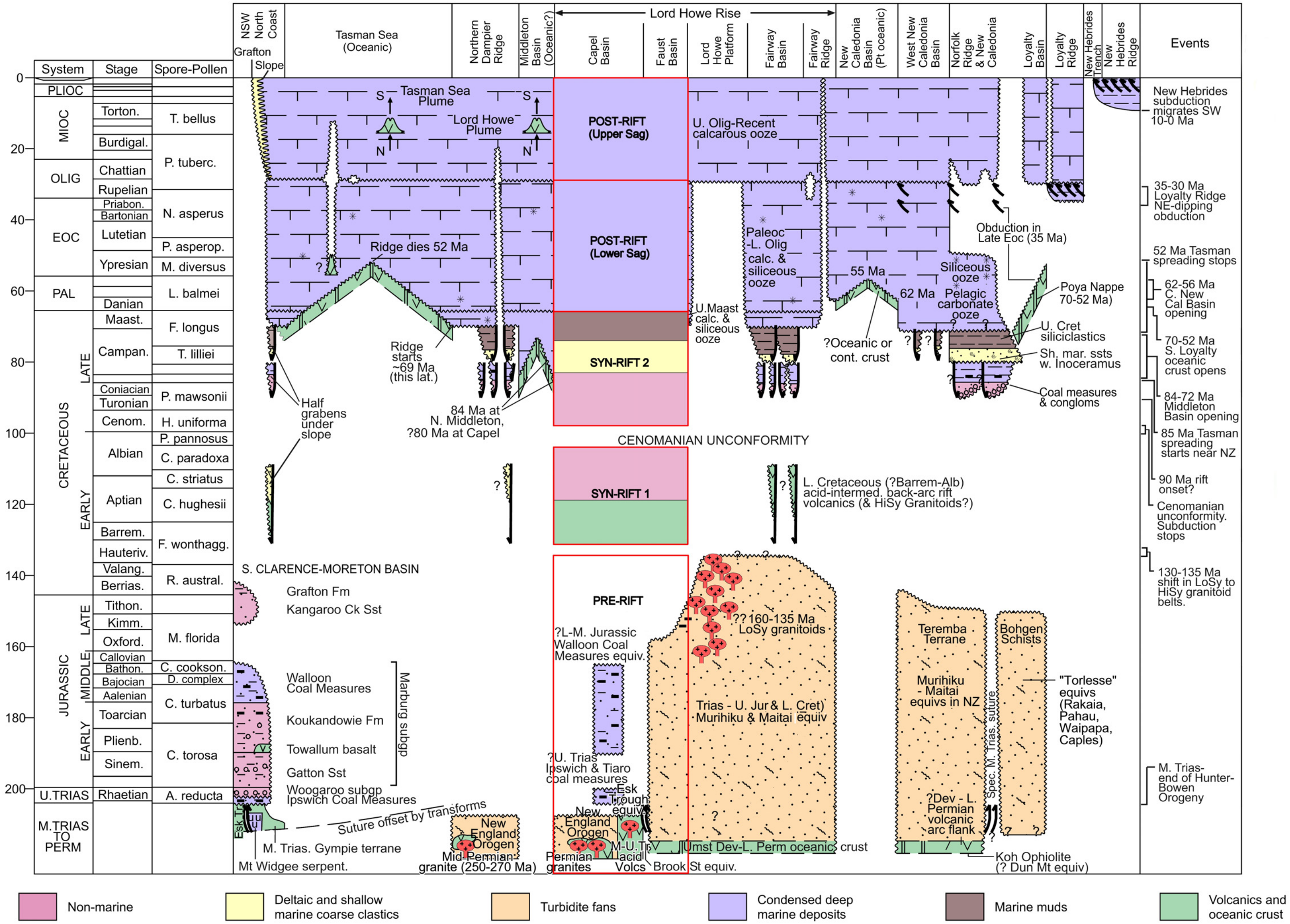

Figure 5: *Mesozoic–Cenozoic regional chronostratigraphic correlation from onshore eastern Australia across the Lord Howe Rise to New Zealand and New Caledonia, showing the inferred positions of the seismic megasequences in the Capel and Faust basins (after Norvick et al., 2008).*

PRE-RIFT BASEMENT

Three seismic facies are recognised within the pre-rift basement: 'layered', 'bland'; and 'volcanic' (see Figures 6 to 11). In many places, the seismic facies laterally grade into each other making their spatial delineation difficult or approximate. Also, it is important to note that the classification of 'layered' or 'volcanic' basement may include early syn-rift rocks where these cannot be clearly distinguished from the pre-rift section on the basis of the present seismic coverage and line orientation.

In a number of places, the basement is vertically composite, made up of a thick 'volcanic' section overlying a 'layered' section. Whether these volcanics are entirely of pre-rift age or include early syn-rift material is conjectural.

'Layered' basement

'Layered' basement (Figure 6) is mainly confined to the northwestern part of the survey area (Figure 7) where it mostly underlies the thickest syn-rift sections. Its seismic character is variable but is typified by low to moderate frequency, low to moderate continuity, sub-parallel to parallel reflectors lying beneath a base syn-rift angular unconformity (horizon CF_Bmtl; Tables 1 and 2). It appears to be sedimentary in origin. The similarity in seismic character with sections of the overlying Syn-rift 1 Megasequence makes picking of the top of 'layered' basement difficult in places. As such, it is possible that some of the identified 'layered' basement includes earliest syn-rift sediments. Regional tectonic reconstructions suggest that it may represent the offshore extension of eastern Gondwanan Mesozoic basins such as the Clarence–Moreton and Maryborough, or the Murihiku Supergroup of New Zealand, and therefore could include potential source rocks such as Jurassic coal measures (e.g. equivalents of the Walloon, Tiaro and Murihiku coal measures; Norvick et al., 2008; Uruski et al., 2008). Penetration into 'layered' basement achieved by the seismic energy source during the GA-302 survey is over 1 second TWT in places; much weaker penetration was achieved by the GA-206 seismic survey because of the smaller energy source.

'Bland' basement

'Bland' basement (Figure 8) is widely distributed in the east of the study area (Figure 9) where it typically forms high-standing, basement blocks and horsts, including the Lord Howe Platform. It commonly contains weak to very weak reflectors and is typically bounded at the top by a high-amplitude reflector (horizon CF_Bmtb; Tables 1 and 2) indicating a lack of penetration by seismic energy (i.e. a hard response). Its upper surface commonly appears to be an old erosional land surface that was planated as it subsided beneath the wave base during the Cenozoic. On many seismic lines, it appears to have remained subaerially exposed until approximately the Oligocene. In several places, younger volcanic features (including volcanic cones and flows) overlie the erosional surface.

This basement type could correspond to a variety of rock types. It could comprise, as has been speculated by Norvick et al. (2008) and Mortimer et al. (2008), correlative rocks of the New England Orogen and/or the Gympie Terrane, or their New Zealand and New Caledonian equivalents. Part of its 'bland' character could be due to induration of the erosional surface or the overlying volcanic rocks, which results in most of the seismic energy being reflected and prevents penetration into the basement rocks. Alternatively, it may reflect a high degree of lithological and structural heterogeneity (e.g. folded metamorphics) or the dominance of non-stratified lithologies (e.g. granite).

'Volcanic' basement

'Volcanic' basement (Figure 10) is very common in the east and south of the seismic grid (Figure 11) where it generally lies between areas of 'bland' basement. It is usually characterised by numerous high-amplitude, discontinuous to chaotic internal reflectors that probably represent volcanic flows, dykes and sills. It many cases, its upper surface (horizon CF_Bmtv; Tables 1 and 2) is broadly mounded, consistent with volcanic build-ups. However, in places, the horizon is difficult to pick due to the occurrence of similar high-amplitude reflectors in the lower part of the overlying Syn-rift 1 Megasequence.

The 'volcanic' basement probably represents volcanic-dominated or highly intruded pre-rift rocks. In parts, it may also represent the earliest syn-rift volcanics (i.e. base of the Syn-rift 1 megasequence) overlying the true pre-rift basement. It may correlate with the earlier part of the Early Cretaceous Grahams Creek Volcanics in the Maryborough Basin or the Whitsunday Volcanic Province of eastern Queensland (Norvick et al., 2008).

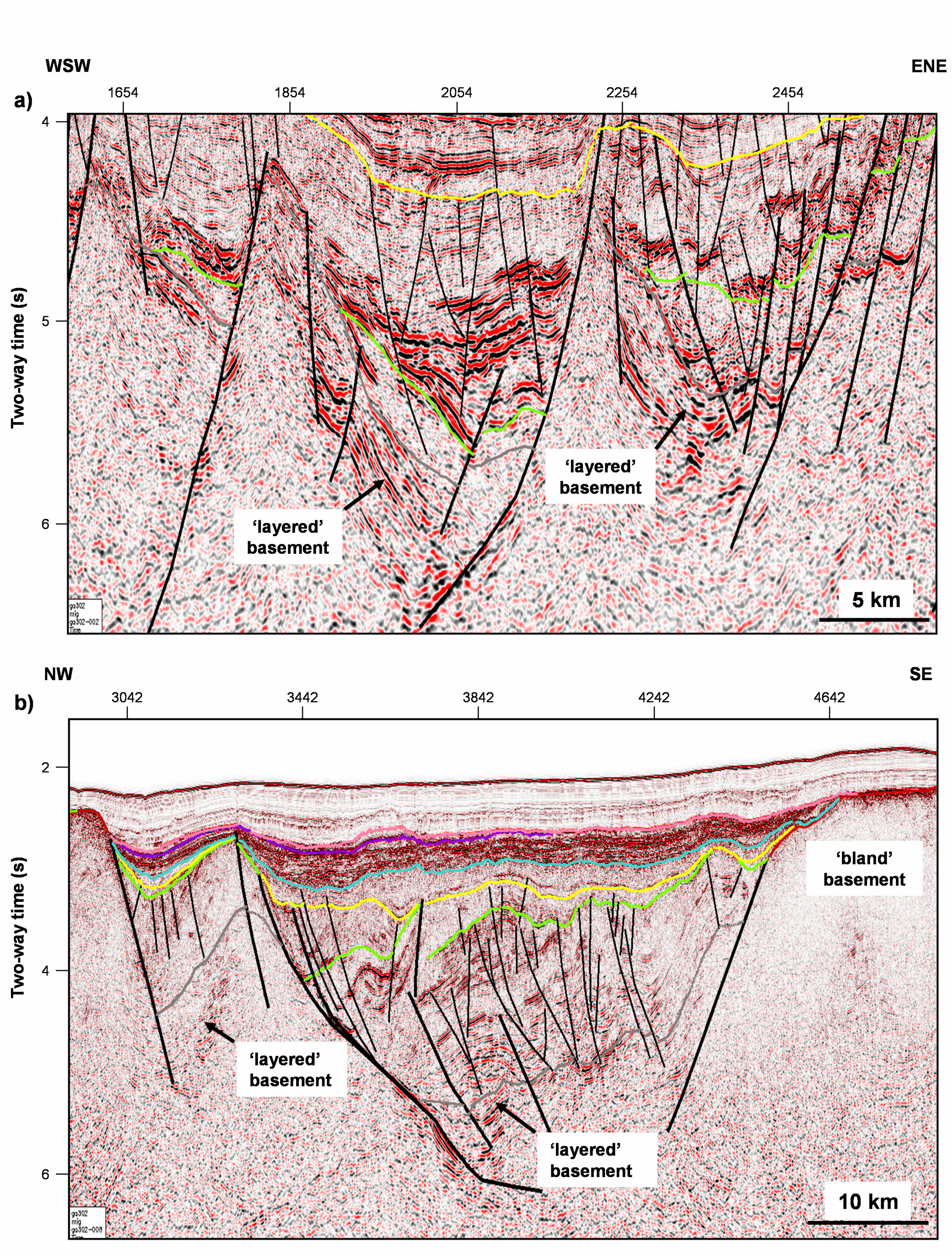

Figure 6: *Examples of 'layered' basement in the seismic data. See Table 1 for identification of the coloured horizons and Figure 7 for the location of the examples.*

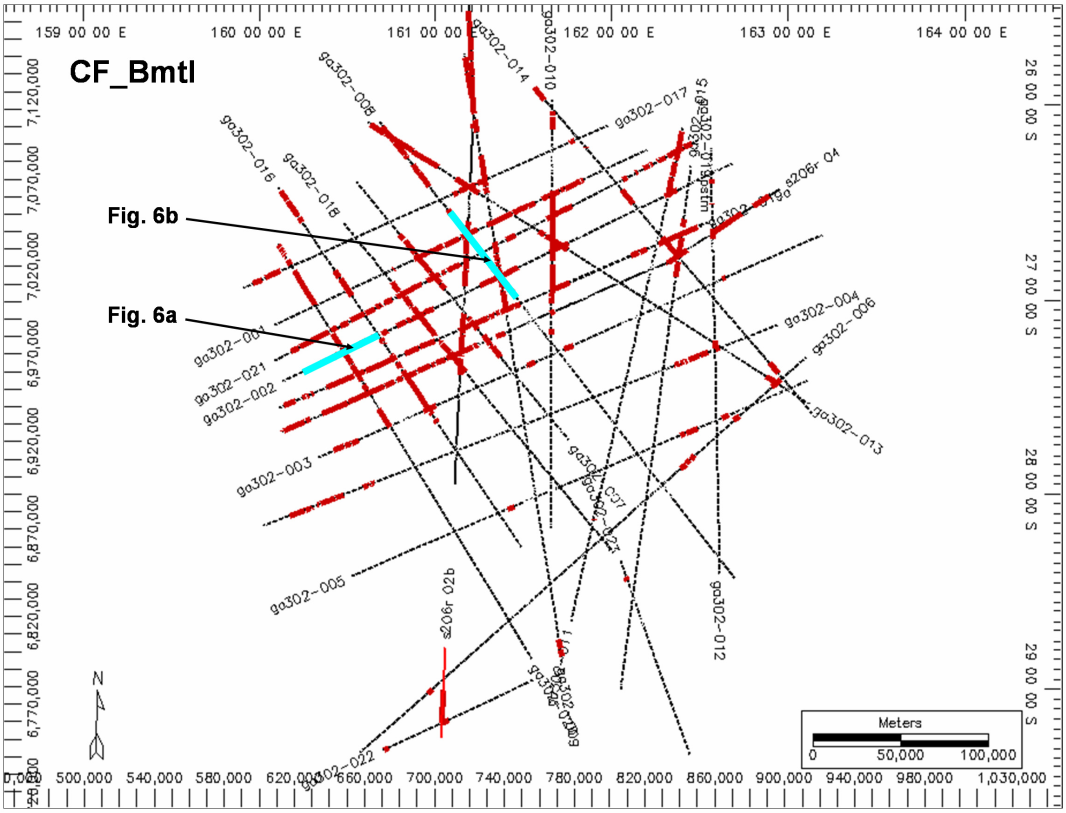

Figure 7: *Map showing the distribution of 'layered' basement along the seismic lines.*

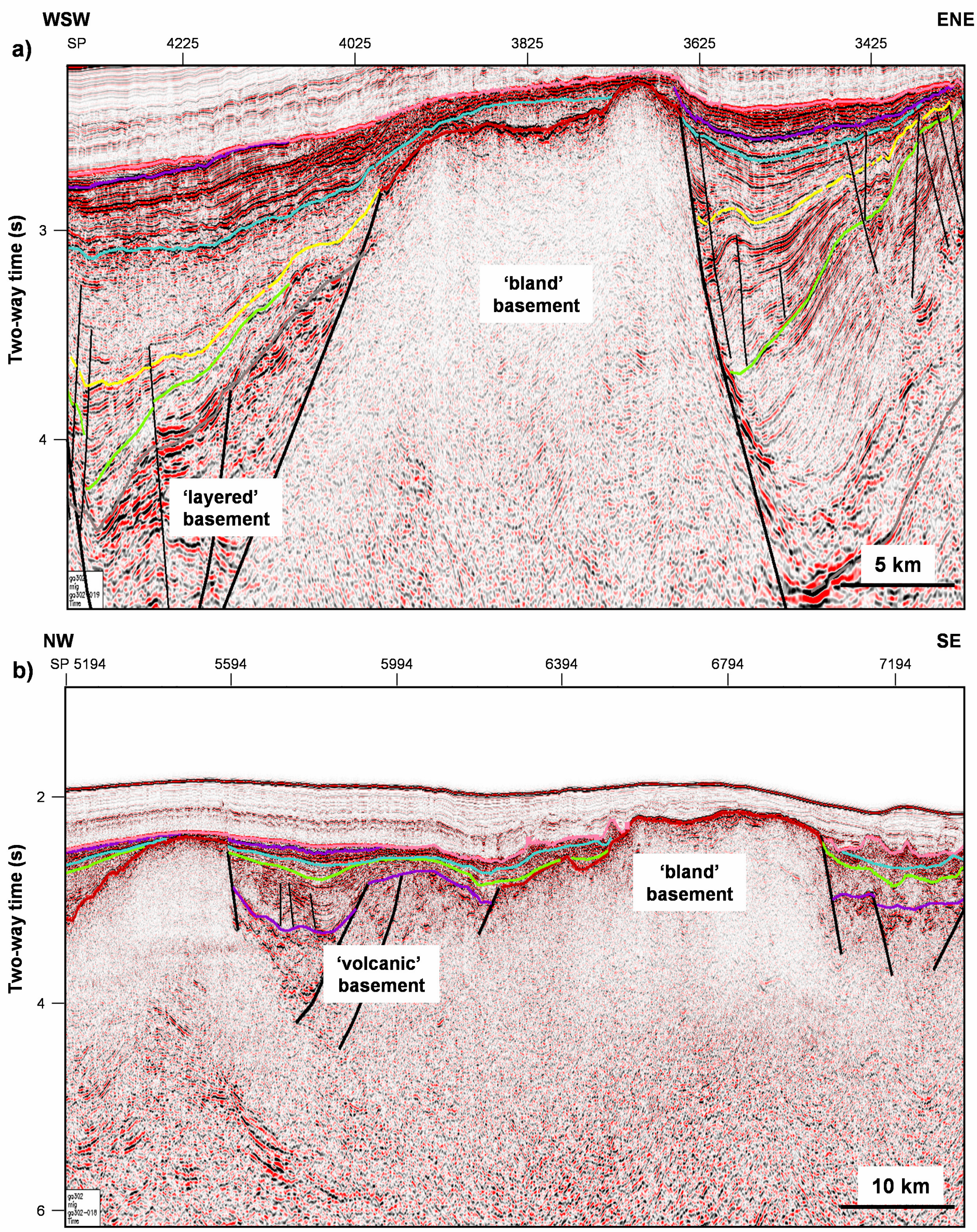

Figure 8: *Examples of 'bland' basement in the seismic data. See Table 1 for identification of the coloured horizons and Figure 9 for the location of the examples.*

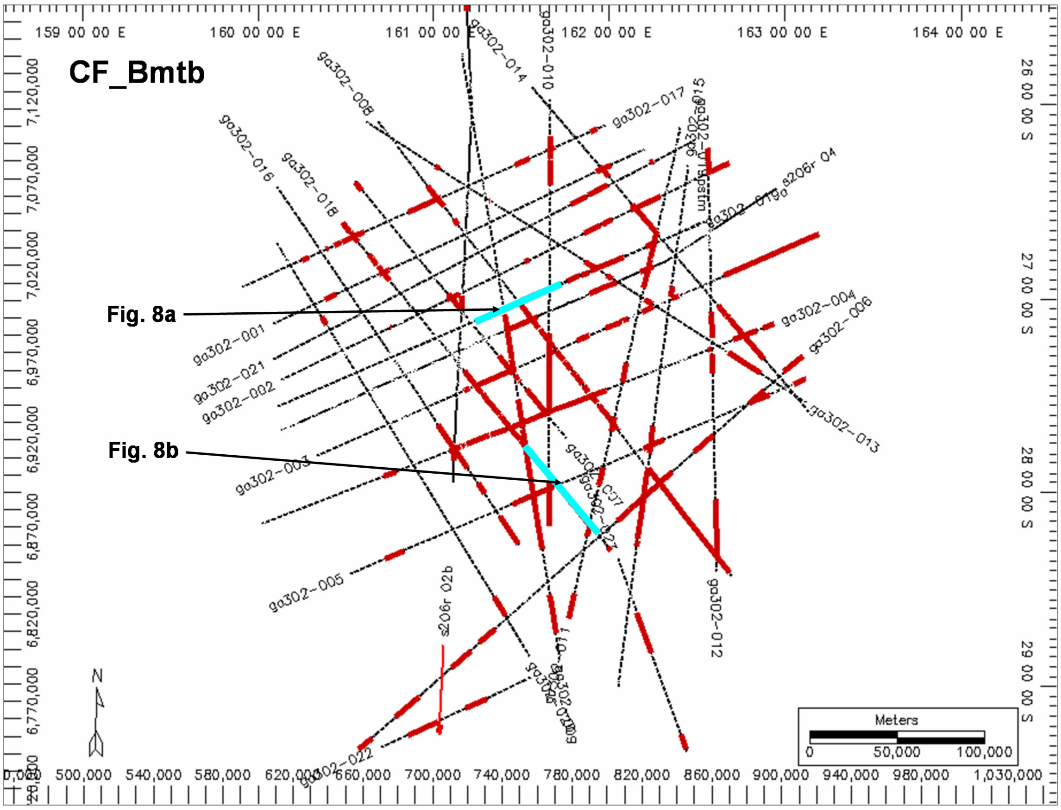

Figure 9: *Map showing the distribution of 'bland' basement along the seismic lines.*

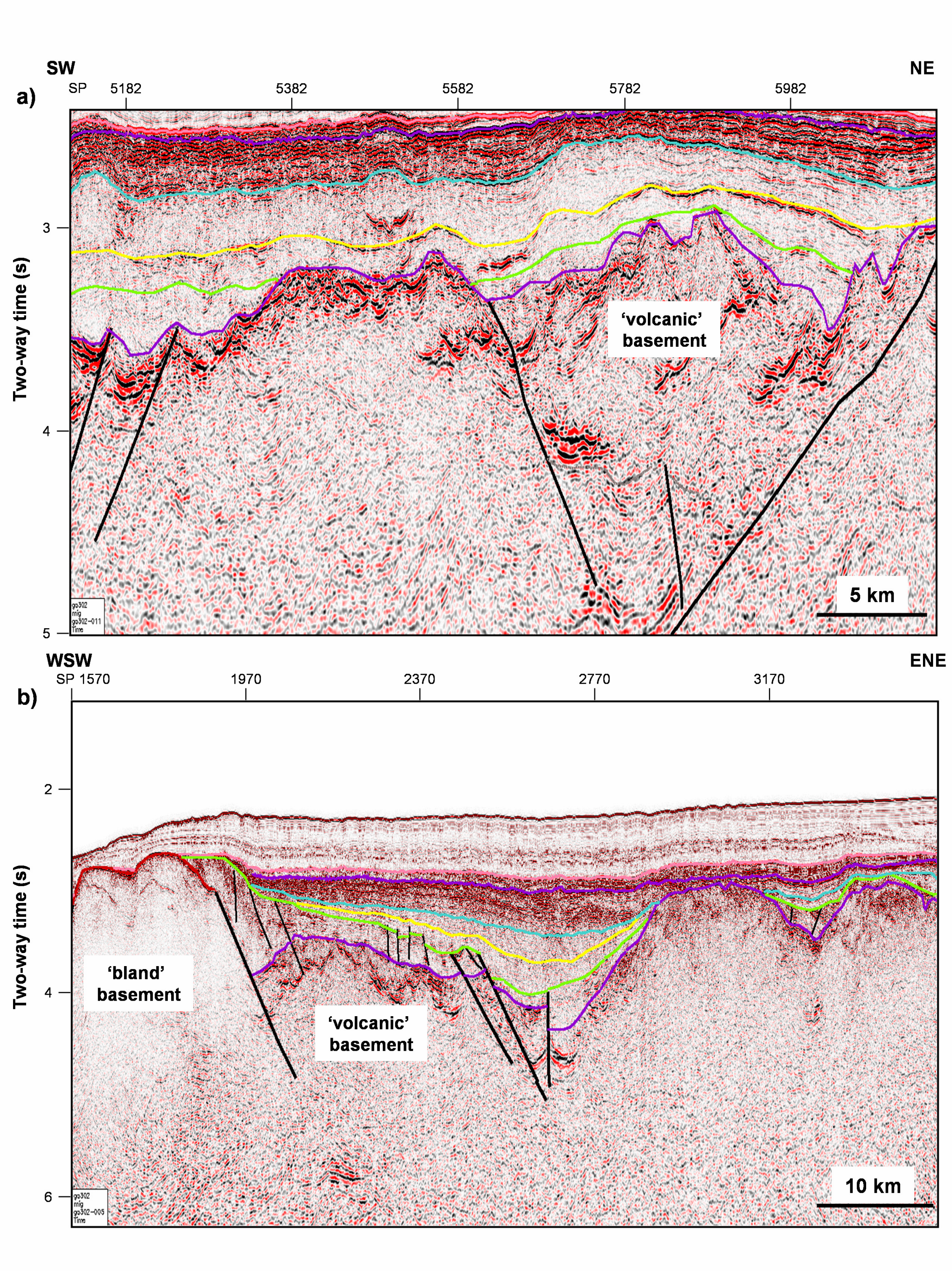

Figure 10: *Examples of 'volcanic' basement in the seismic data. See Table 1 for identification of the coloured horizons and Figure 11 for the location of the examples.*

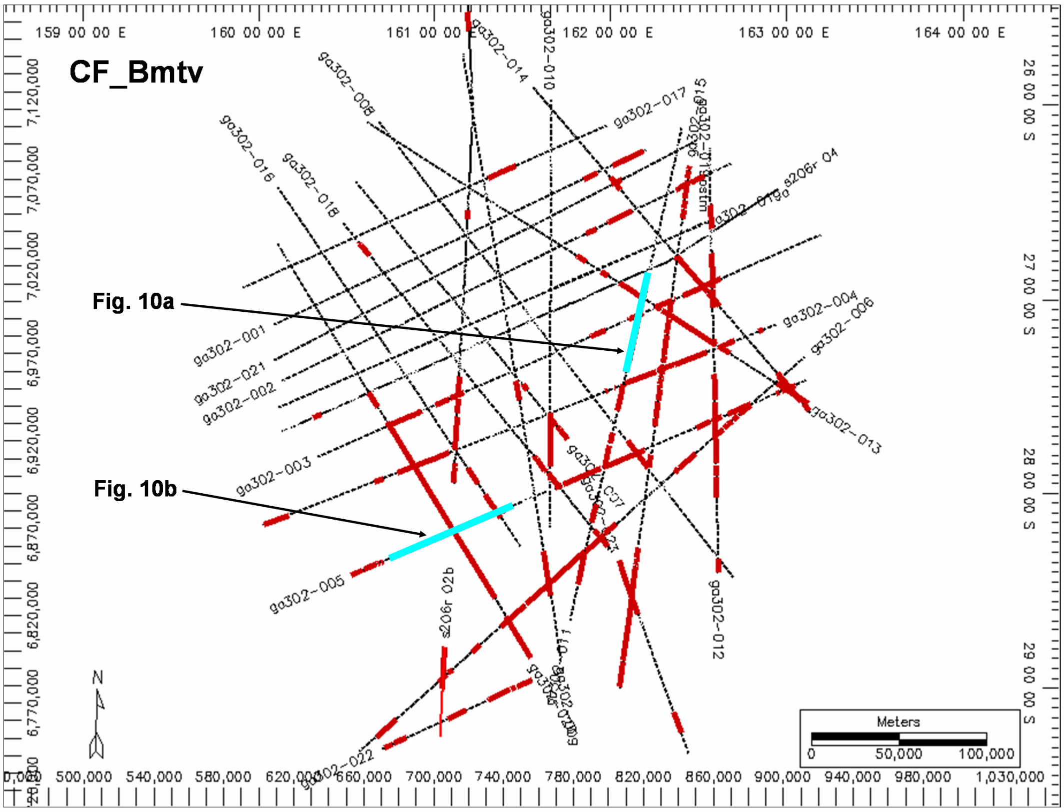

Figure 11: *Map showing the distribution of 'volcanic' basement along the seismic lines.*

SYN-RIFT 1 MEGASEQUENCE

Total (syn- plus post-rift) sediment thickness in the Capel and Faust basins reaches 3.6 seconds TWT (Figure 12). By definition, this excludes the sedimentary section within the 'layered' pre-rift basement.

The Syn-rift 1 Megasequence (Figures 4 and 13) represents the first major phase of rifting in the basins, possibly in the Early Cretaceous. It is bounded at its top by a major regional unconformity (horizon CF_Sr1B; Tables 1 and 2) of postulated Cenomanian age (Norvick et al., 2001, 2008). The megasequence is up to 2.2 seconds TWT thick with the thickest section occurring in depocentres (grabens and half-grabens) in the central northern part of the study area (Figure 14). In the northwest, the megasequence is highly faulted beneath the Syn-rift 2 Megasequence (Figure 4).

The Syn-rift 1 Megasequence has an extremely variable seismic character, ranging from bland, chaotic to layered. The low reflector continuity and the fluctuating reflector amplitude and frequency are consistent with rapid lateral and vertical facies changes in lithology. The megasequence includes numerous local unconformities which cannot be carried from one depocentre to the next.

It is likely that the Syn-rift 1 Megasequence is dominated by non-marine clastic and volcaniclastic sediments, mostly of fluvial origin and possibly with a tuffaceous component. Areas of bland seismic character may equate to coarse-grained channel and fan deposits, while chaotic seismic character may indicate mass movement deposits, possibly associated with volcanic activity. It also appears to include numerous volcanic flows, dykes and sills. The megasequence is probably the product of complex interplay between volcanism and non-marine deposition in developing, highly compartmentalised rift depocentres. Sediment was presumably transported by fluvial and mass movement processes from local source areas on the flanking highs via ramps or faulted boundaries of the rift depocentres.

On seismic lines in the central western part of the study area, a distinct basal seismic package (designated Syn-rift 1A in Table 3) has been identified within the Syn-rift 1 Megasequence (Figures 13 and 15). This package is bounded at the top by an unconformity (CF_Sr1A seismic horizon; Tables 1 and 2) and is mainly confined to the major depocentres in the central part of the study area. It is typically characterised by high-amplitude, low-frequency and moderate-continuity reflectors that possibly represent coal and volcanics interbedded with clastic non-marine sediments. Coal may have been deposited in a paludal environment that developed with faulting in the early stages of rifting, conditions which may also have been favourable for lacustrine deposition.

The Syn-rift 1 Megasequence may represent the equivalent of the ?Aptian–Albian succession of the Whitsunday Volcanic Province (Bryan et al., 1997, 2000) or the Early Cretaceous volcaniclastic successions distributed widely in eastern Australia from the Surat and Eromanga basins southward to the Gippsland (Strzelecki Group), Bass (Otway Megasequence) and Otway (Eumeralla Supersequence) basins (Norvick et al., 2001, 2008; Krassay et al., 2004; Blevin et al., 2005). The Aptian–Albian Maryborough Formation and Burrum Coal Measures in the Maryborough Basin may also be a correlative, although deposition here took place under a sag, rather than syn-rift, regime (Ellis, 1968; Hill, 1994; Stephenson and Burch, 2004).

The unconformity at the top of the Syn-rift 1 Megasequence is likely to be an expression of the Cenomanian uplift and erosion event widely documented from eastern Australia (e.g. Hill, 1994; Raza et al., 2009) that may be attributable to a major reorganisation of the Australia–Pacific plate boundary (Veevers, 2000; Norvick et al., 2001, 2008; Willcox et al., 2001; Schellart et al., 2006; Rey and Müller, 2010) and, possibly, the emplacement of a mantle plume (Crawford et al., 2003).

SYN-RIFT 2 MEGASEQUENCE

The Syn-rift 2 Megasequence (Figures 4 and 16) unconformably overlies Syn-rift 1. In contrast to the Syn-rift 1 Megasequence, it thickens towards the northwest of the study area (Figure 17) where it typically exhibits growth into major westerly-dipping faults (Figures 4 and 16). Here it reaches a maximum thickness of over 1.4 seconds TWT (Figure 17). In other parts of the seismic grid, the megasequence is generally less than 0.5 seconds TWT thick and commonly displays sag geometries rather than syn-rift relationships. However, it is up to 0.6 seconds TWT thick in a north–south elongated zone of sag deposition in the Faust Basin (Figure 17), in the eastern part of the seismic grid.

In the major depocentres, the megasequence is generally characterised by parallel to divergent, moderate to high-amplitude reflectors with moderate continuity and frequency. Packages of clinoformal reflectors are also observed in some places. Elsewhere, particularly in the east and south of the study area, it has a bland appearance containing only weak sub-parallel reflectors. It is bounded at its top by a regional unconformity (horizon CF_Sr2B). Regional tectonostratigraphic reconstructions suggest that this horizon is the breakup unconformity associated with the opening of the Tasman Sea and the Middleton Basin during the Campanian (Norvick et al., 2001, 2008).

The megasequence is interpreted to be dominated by fluvial to marginal marine (toward the top of the megasequence in the western parts of the study area) clastic sediments. Areas of bland seismic character may represent bedload-dominated fluvial channel and alluvial fan deposits. Clinoformal reflectors suggest deltaic deposition, triggered by marine incursion in the latter part of rifting or, alternatively, within lakes. Lateral and vertical variations in the reflector amplitude are probably related to spatio-temporal transitions in the deposition of fine and coarse-grained facies, such as that seen in alluvial and deltaic systems. At its base, the megasequence commonly includes a package of high-amplitude, sub-parallel to chaotic, discontinuous reflectors (seismic package Sr2A; Table 3, Figures 16 and 18), which are interpreted to be dominated by volcanic and intrusive rocks. This episode of magmatism probably marks the start of a renewed phase of extension with a westerly locus that eventually led to the opening of the Tasman Sea and the Middleton Basin, and resulted in the creation of major accommodation space for the megasequence. Volcanic and volcaniclastic rocks dredged from the eastern Lord Howe Rise and Fairway Ridge during the AUSFAIR survey (Colwell et al., 2006) have yielded Late Cretaceous zircon-derived ages (Higgins et al., in press), and probably represent correlatives of the Syn-rift 2 Megasequence.

Similar megasequences have been identified from other Cretaceous rift basins of the former eastern Gondwana margin. Probable Cenomanian–Campanian non-marine to shallow marine syn-rift successions have been identified from the Gower Basin on the central Lord Howe Rise (Willcox and Sayers, 2002), and the southern Lord Howe Rise (Stagg et al., 2002). In both areas, deposition has been related to the extension associated with the rifting of the Tasman Sea, which was accompanied by substantial magmatism (McDougall and van der Lingen, 1974; Gaina et al., 1998; Stagg et al., 2002; Willcox and Sayers, 2002). Late Cretaceous syn-rift deposition is also recorded over the Norfolk and West Norfolk ridges (Herzer et al., 1997, 1999; Mortimer et al., 1998), in the Northland Basin (Uruski and Baillie, 2004; Uruski et al., 2008) and in the Reinga Basin (Herzer et al., 1997, Stagpoole et al., 2009).

The Syn-rift 2 Megasequence may correlate with the Turonian–Campanian Emperor and Golden Beach subgroups of the Gippsland Basin (Bernecker and Partridge, 2001; Bernecker et al., 2001), the Albian–Campanian Taniwha and Rakopi formations of the Taranaki Basin (King and Thrasher, 1996; Uruski and Baillie, 2004), and the Turonian–Santonian Hoiho Group of the Great South and Canterbury basins (Killops et al., 1997; Cook et al., 1999; Uruski and Baillie, 2001). The timing and environment of deposition vary due to regional diachronicity in the onset and termination of rifting. However, all of these successions contain coaly potential hydrocarbon source rocks, some of which are oil prone (Killops et al., 1997; Cook et al., 1999).

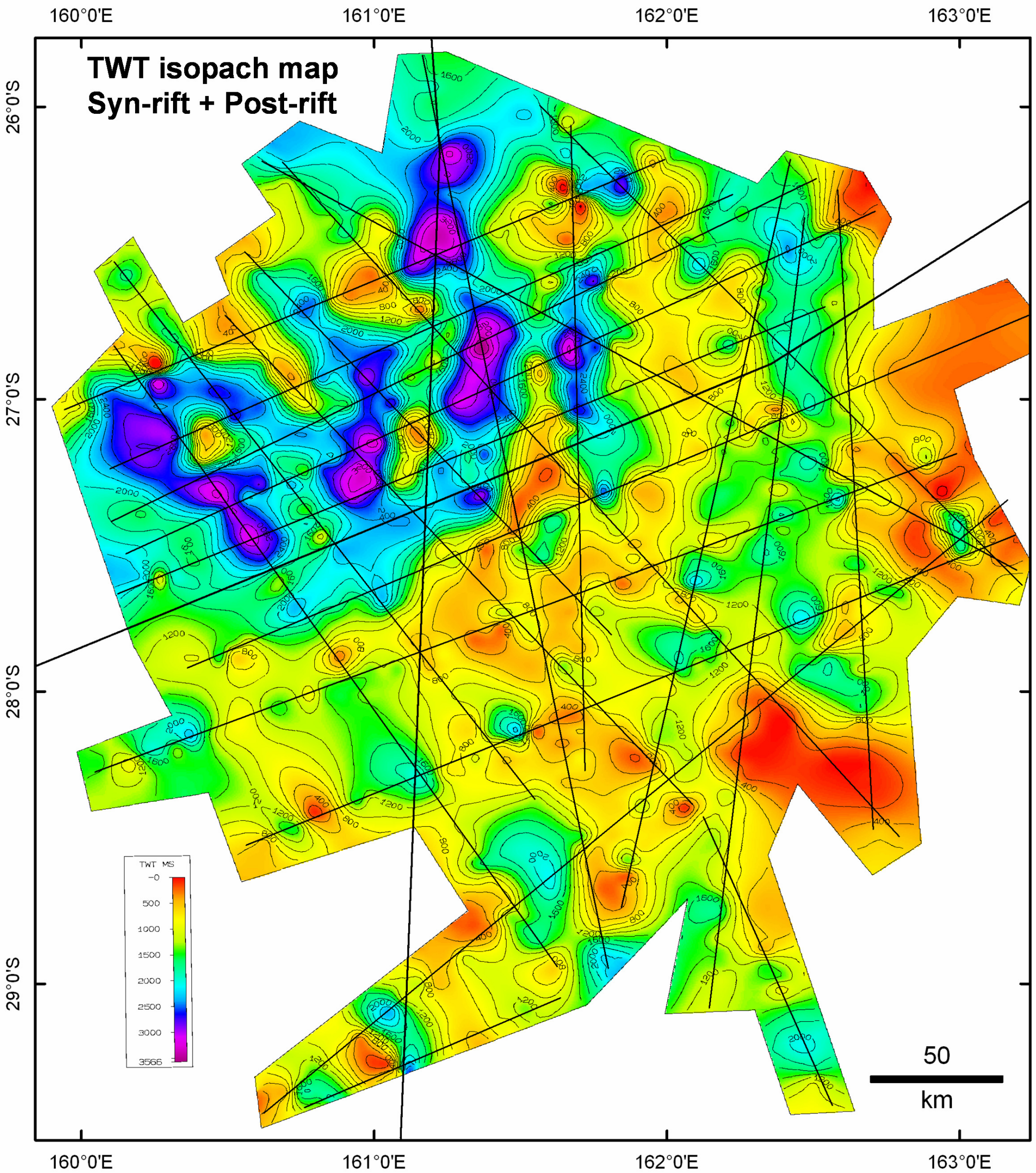

Figure 12: *Map showing the total sediment thickness in milliseconds TWT. The map is generated from the seismic horizons CF_Wb and CF_CretRift (see Table 1). It is the sum of the thicknesses of the Syn-rift 1, Syn-rift 2 and Post-rift megasequences (see Tables 2 and 3). It excludes any pre-rift sedimentary section within 'layered' basement.*

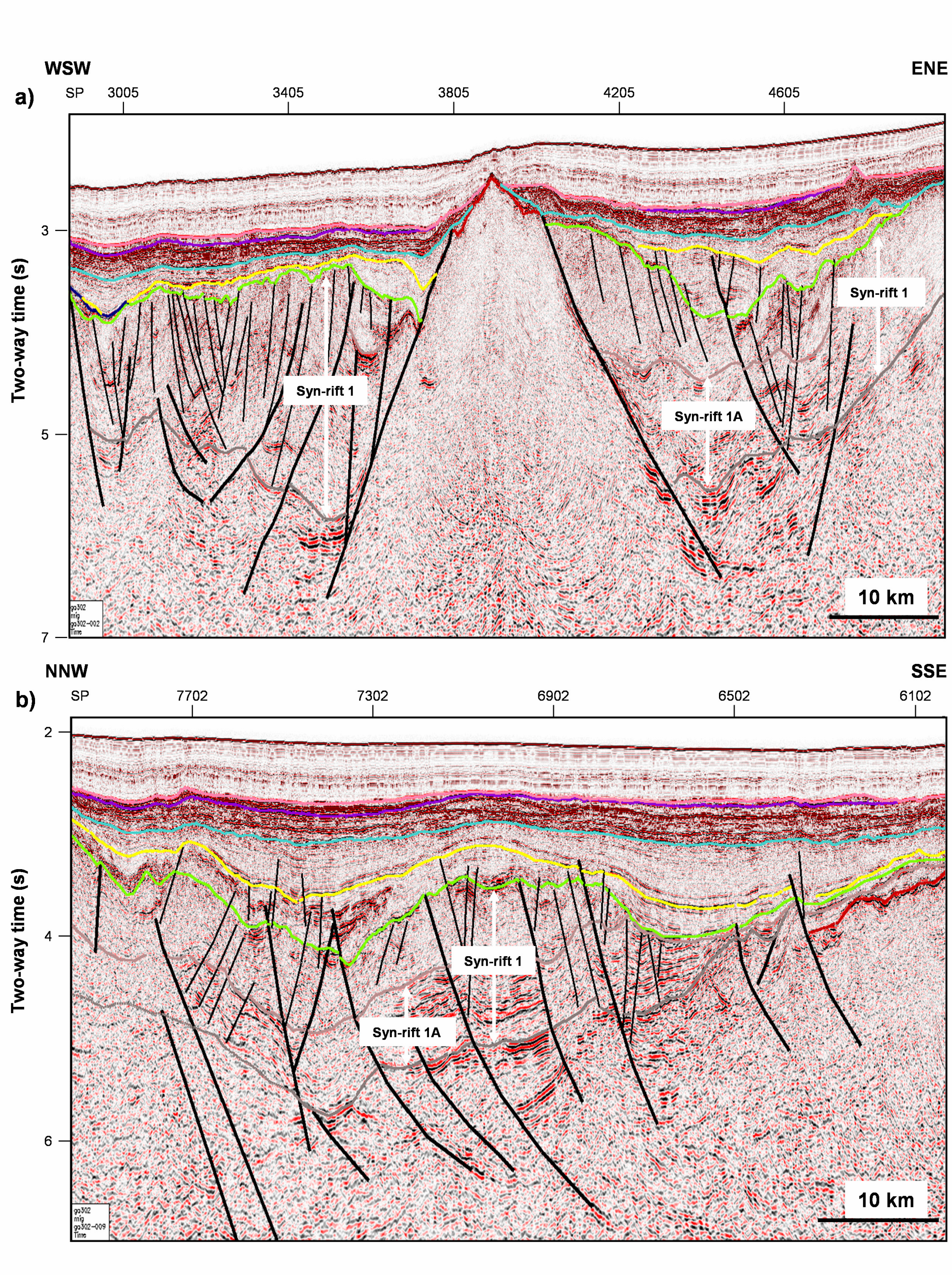

Figure 13: *Examples of the Syn-rift 1 Megasequence in the seismic data. See Table 1 for identification of the coloured horizons and Figure 14 for the location of the examples.*

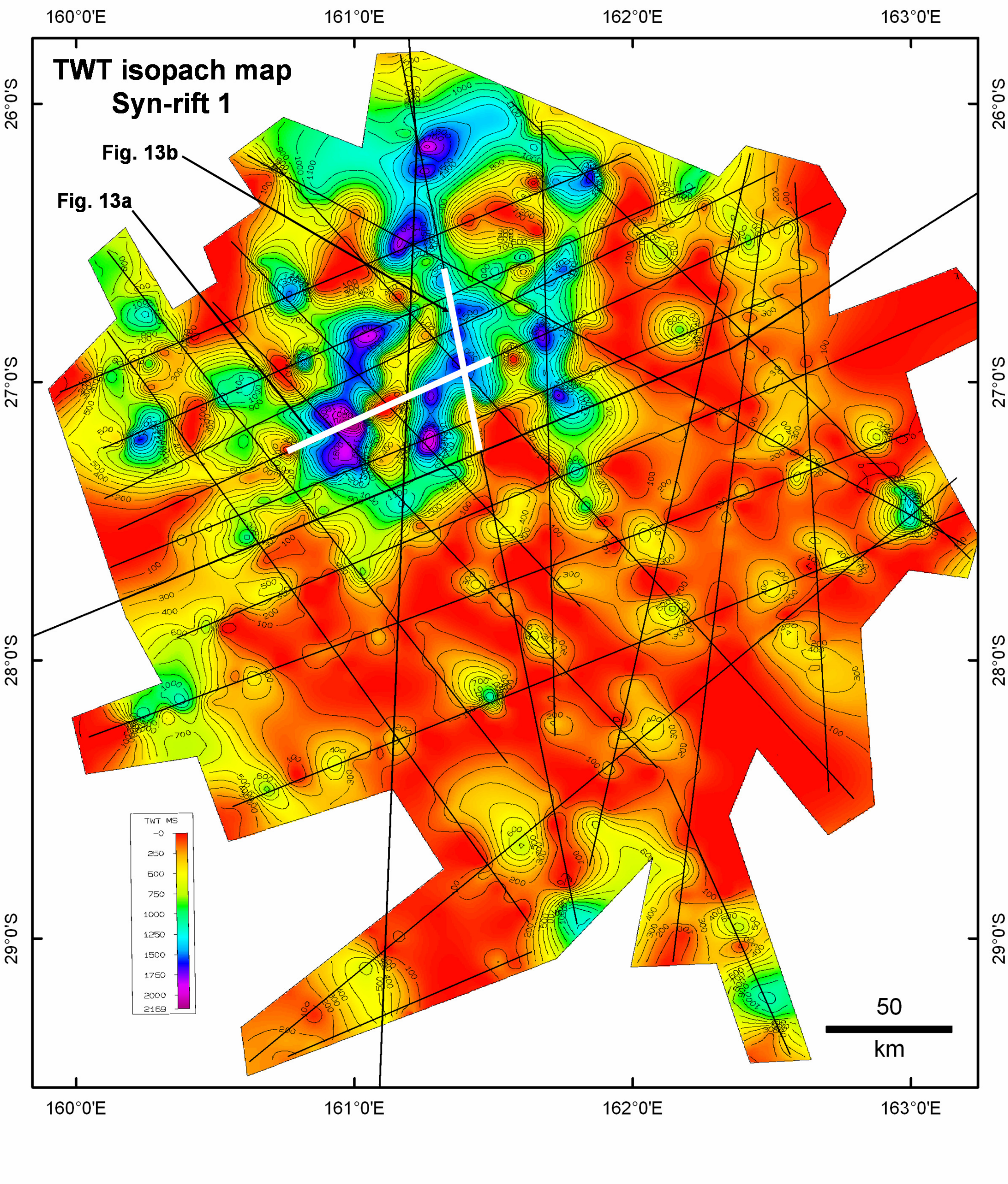

Figure 14: *Map showing the thickness of the Syn-rift 1 Megasequence in milliseconds TWT. The map is generated from the seismic horizons CF_CretRift and CF_Sr1B (see Table 1).*

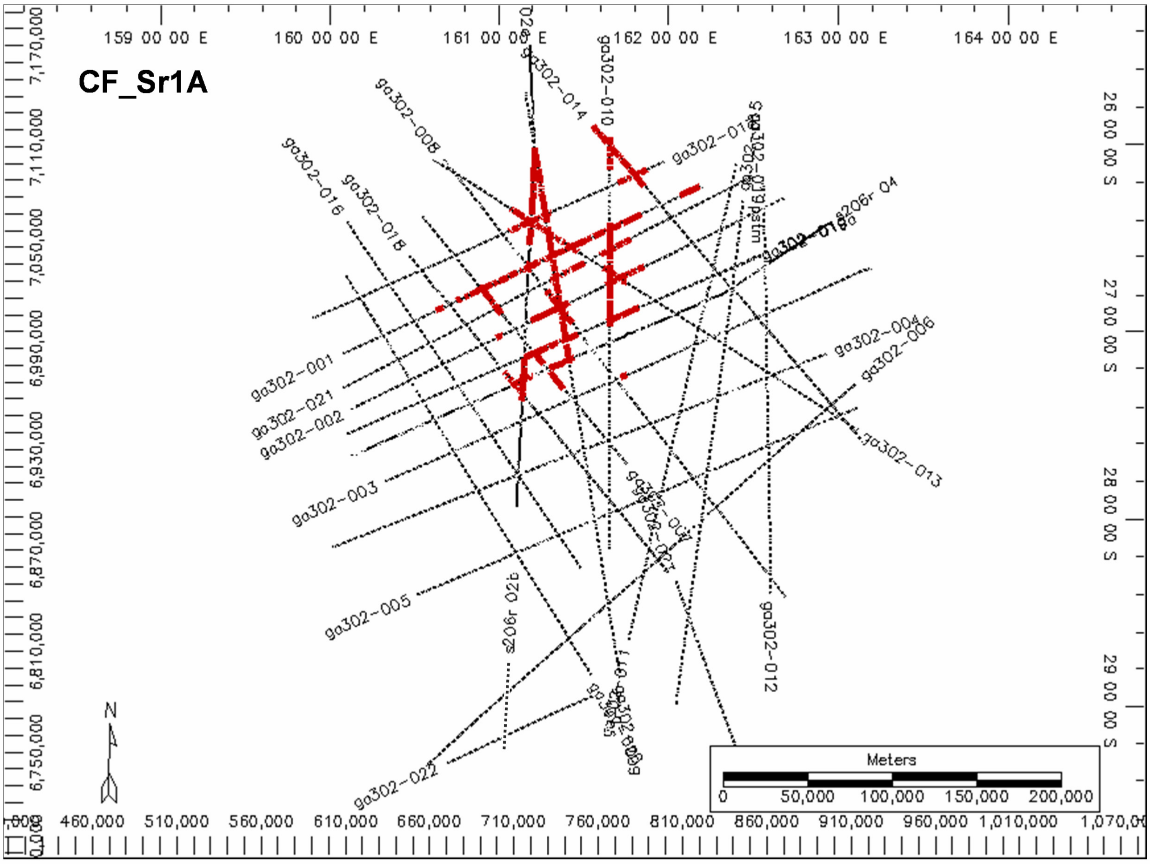

Figure 15: Map showing the distribution of seismic package Syn-rift 1A along the seismic lines.

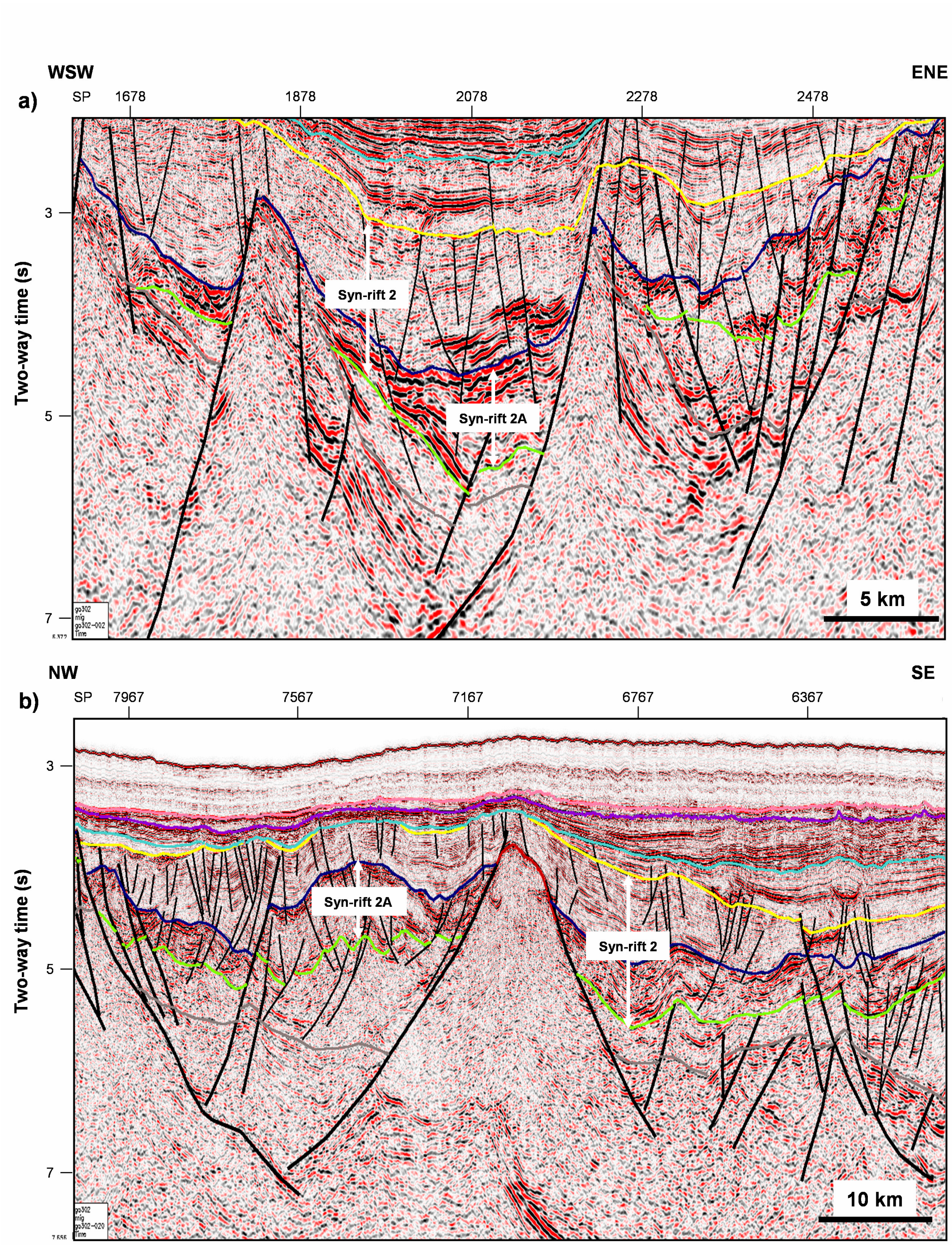

Figure 16: *Examples of the Syn-rift 2 Megasequence in the seismic data. See Table 1 for identification of the coloured horizons and Figure 17 for the location of the seismic examples.*

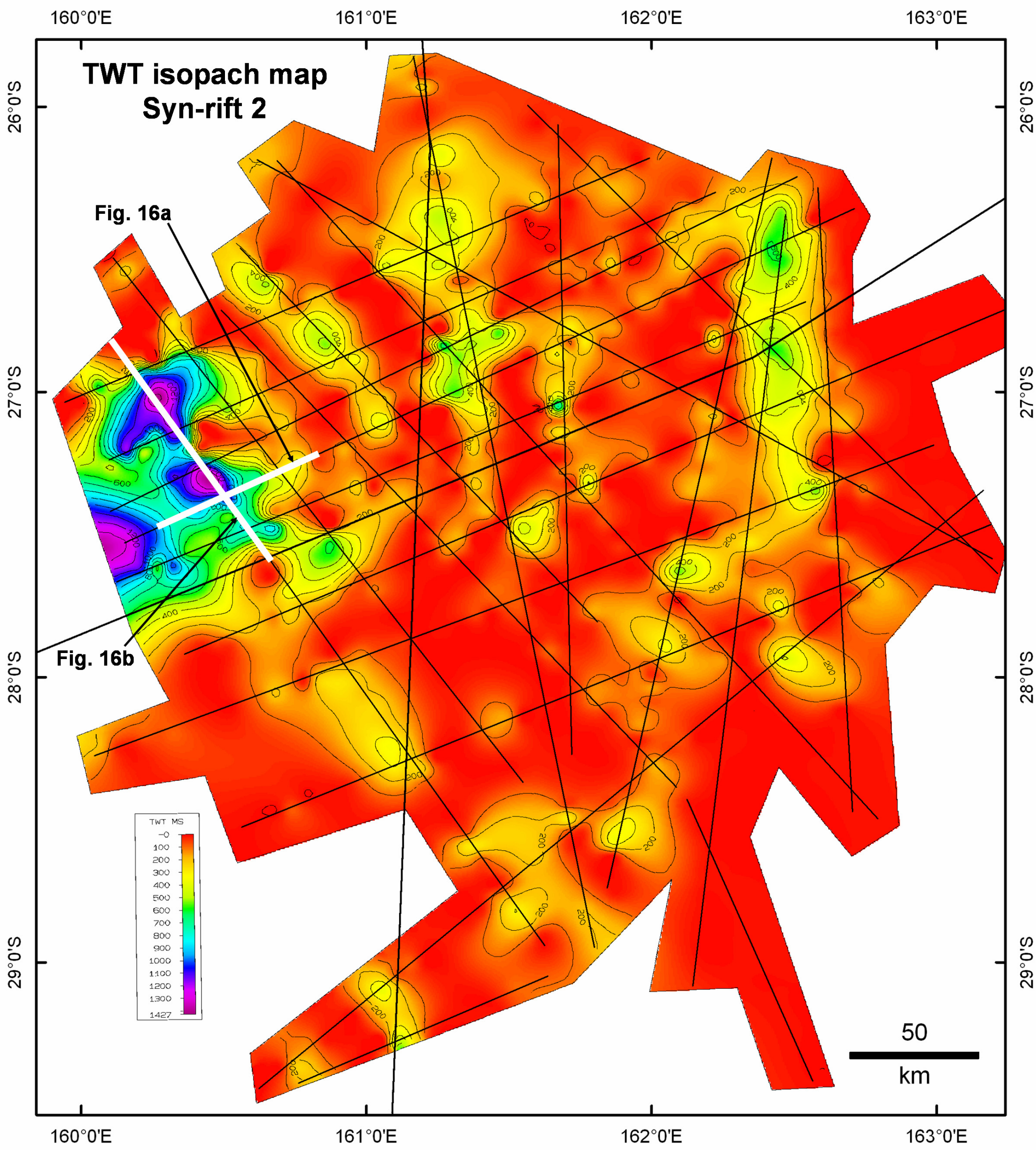

Figure 17: *Map showing the thickness of the Syn-rift 2 Megasequence in milliseconds TWT. The map is generated from the seismic horizons CF_Sr1B and CF_Sr2B (see Table 1).*

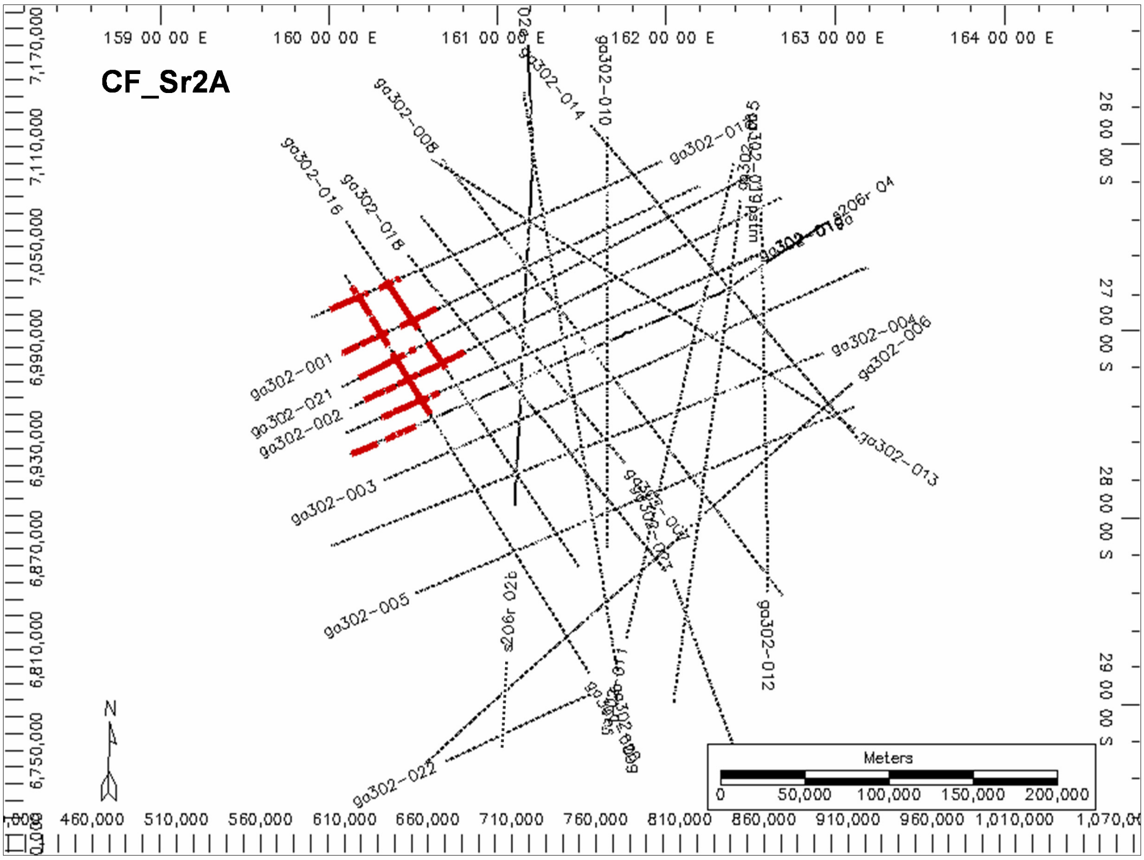

Figure 18: *Map showing the distribution of seismic package Syn-rift 2A along the seismic lines.*

POST-RIFT MEGASEQUENCE

The Post-rift Megasequence (Figures 19 and 20) is less structured than the underlying syn-rift megasequences and represents deposition during the post-rift thermal subsidence phase. It is up to 1.8 seconds TWT thick. Maximum thickness is attained in depocentres in the central western part of the study area (Figure 21), in many cases coinciding with the areas of the thickest syn-rift deposits (see Figures 14 and 17).

The megasequence can be split into two major seismic packages, namely Lower Sag of probable Campanian to Late Maastrichtian age, and Upper Sag of Late Maastrichtian to Recent age (Figure 20a). The Upper Sag section contains two regional unconformities (CF_Eoc and CF_Olig, Table 1), both dated in the DSDP hole 208.

Seismically, the Lower Sag is characterised by parallel to divergent (rarely clinoformal) reflectors of variable frequency and amplitude, but may have a bland appearance in places (Figure 20). The section is interpreted to consist of siliciclastic to calcareous sandstones and mudstones of marginal marine to neritic origin, grading upward to finer-grained bathyal sediments (Table 3). Moundforms seen in places probably indicate turbidite fans.

In contrast, the Upper Sag section is characterised by parallel, high-frequency reflectors. There is a marked decrease in the amplitude of reflectors across the CF_Olig unconformity, from high amplitude in the lower section to low in the overlying section (Figure 20b). The reasons for this change in amplitude are unclear, but in DSDP hole 208, it appears to correspond to an increasing siliceous component in the deeper section (The Shipboard Scientific Party, 1973c).

Based on the DSDP data and seismic character, the Upper Sag is interpreted to consist mainly of siliceous and calcareous chalk, marl and chert passing above the CF_Olig horizon into calcareous foraminiferal and nannofossil chalk and ooze. The vast majority of the rocks were deposited in an open-marine environment. Coastal, shoreline and shallow marine environments may have existed around emergent basement highs (islands) that finally subsided below wave base, commonly after the Oligocene.

Significant amounts of volcanic rocks appear to be present at various levels in the Upper Sag section. These are particularly common about the CF_Eoc stratigraphic level. Volcanic cones extend to the seafloor in places; some of these were dredged during the GA-2436 marine survey in 2007 (Heap et al., in prep.). Other features that are present in the Upper Sag section include possible mud volcanoes, extensive polygonal faulting probably related to dewatering of the pelagic sediments (Figure 20) and a possible reef (see Appendix 2).

A cross-cutting bottom simulating reflector (BSR) of possible diagenetic origin has been identified in a few places (Figure 22). BSRs were initially identified on seismic data over the Lord Howe Rise and the Fairway Basin in the 1990s. Several workers postulated that these reflectors indicated extensive deposits of methane hydrates within Cenozoic sediments, leading to speculations of a vast untapped petroleum resource underlying the seafloor of the region (Ramsay et al., 1997; Exon et al., 1998; Lafoy et al., 1998a, 1998b; Bernardel et al., 1999; Auzende et al., 2000b, 2000c; Exon et al., 2004, 2007). Work since the mid-2000s, including the results of the 2006 AUSFAIR survey (Colwell et al., 2006), has indicated, however, that the BSRs is most likely to be of diagenetic origin related to the Opal-A/Opal-CT transition front (Nouzé et al., 2005, 2009).

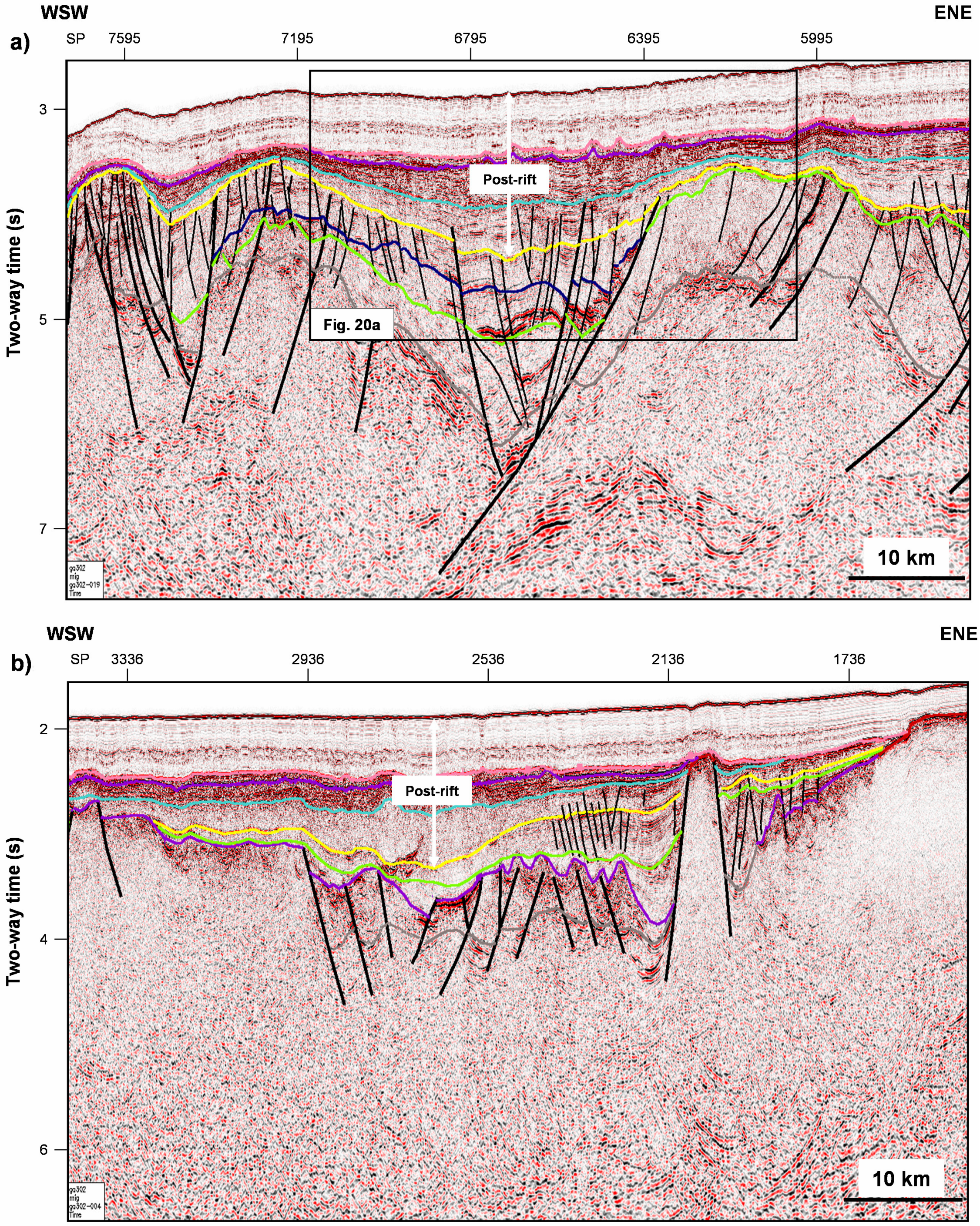

Figure 19: *Examples of the Post-rift Megasequence in the seismic data. See Table 1 for identification of the coloured horizons and Figure 21 for the location of the seismic examples.*

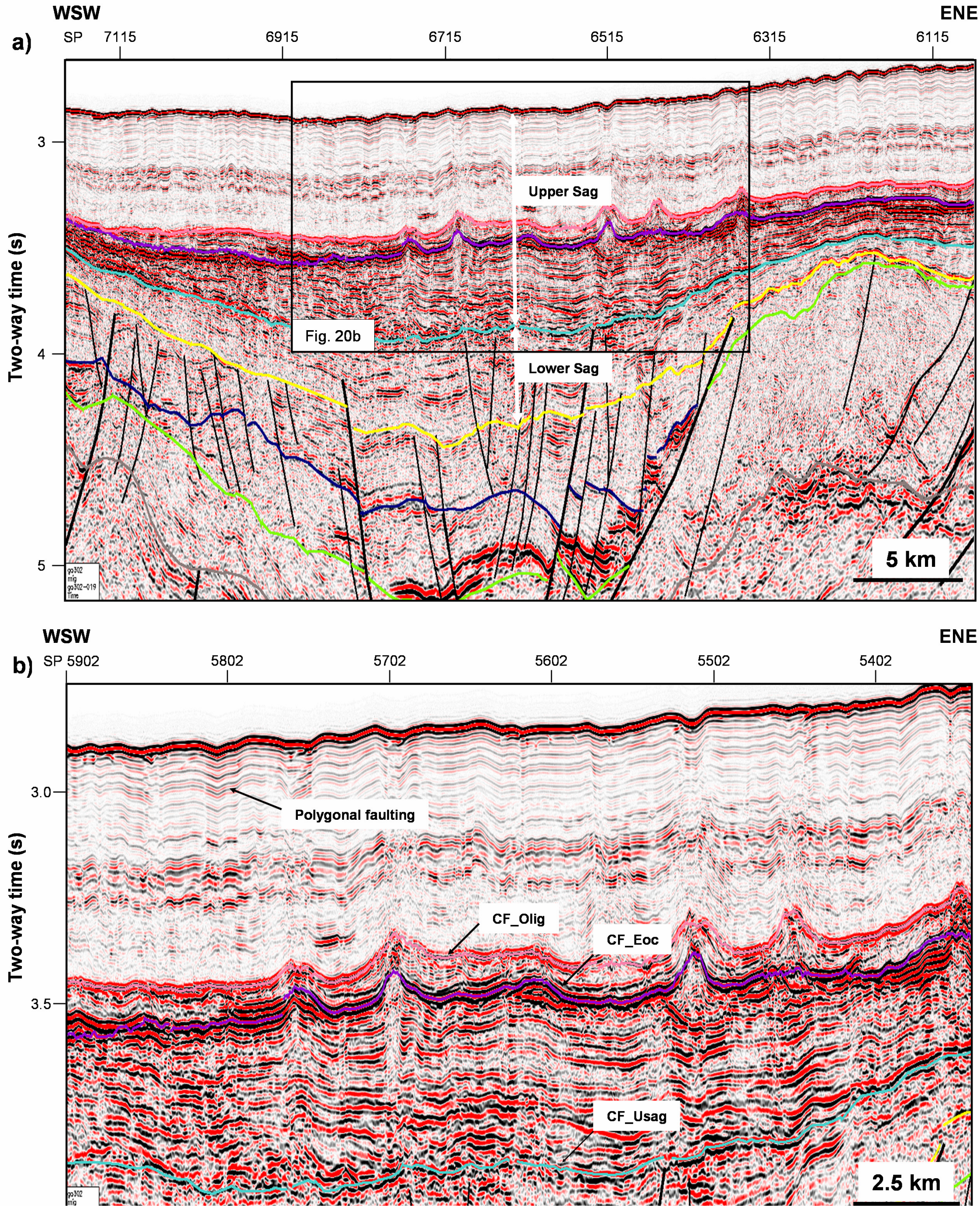

Figure 20: *Detailed examples of the Post-rift Megasequence in the seismic data showing (a) the division into Upper Sag and Lower Sag packages separated by horizon CF_Usag (light blue), and (b) probable dewatering features and polygonal faulting in the upper part of the section above the CF_Olig (pink) horizon. A description of probable mud volcanoes at about the CF_Olig (pink) horizon is given in Appendix 2. See Table 1 for identification of the coloured horizons and Figure 19 for the location of the examples.*

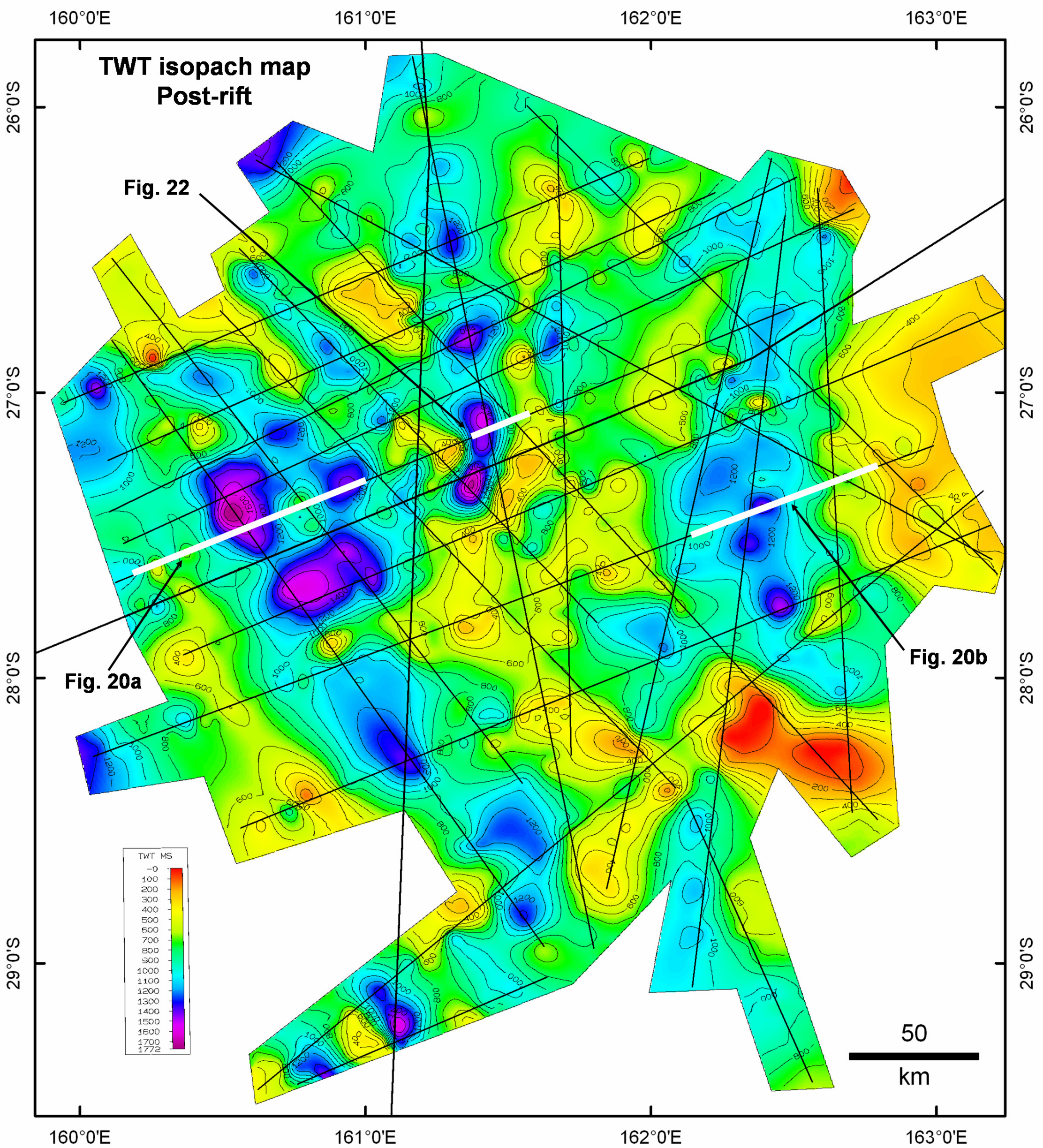

Figure 21: *Map showing the thickness of the Post-rift Megasequence in milliseconds TWT. The map is generated from the seismic horizons CF_Sr2B and CF_Wb (see Table 1).*

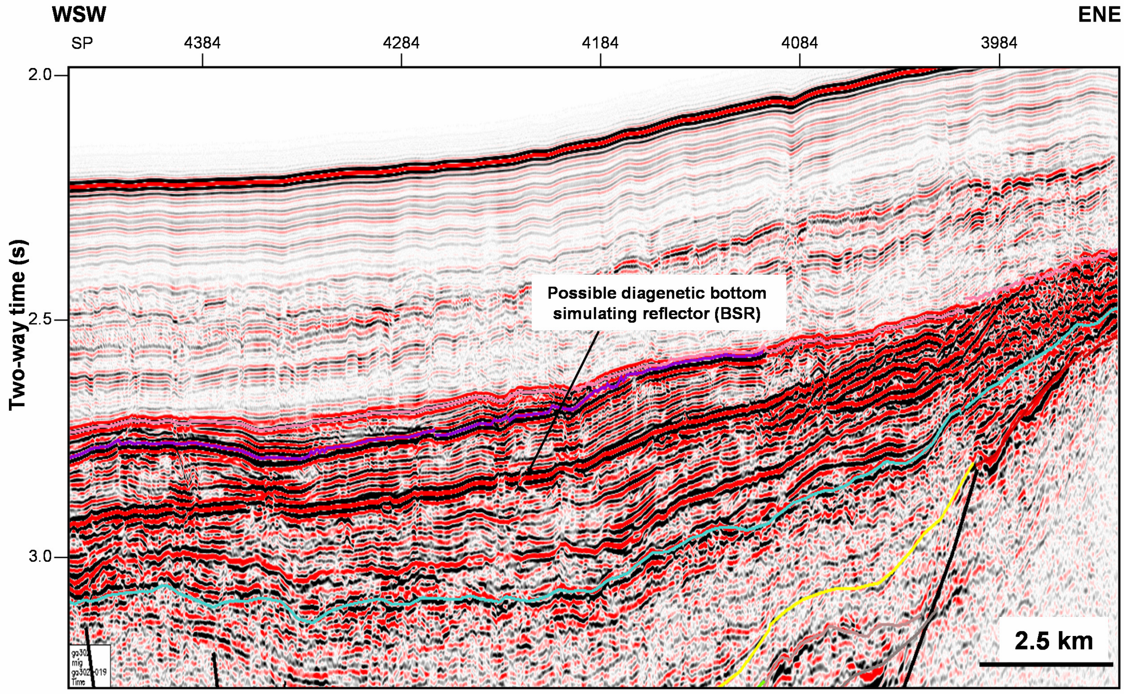

Figure 22: *Example of a possible diagenetic bottom simulating reflector (BSR) within the Upper Sag section of the Post-rift Megasequence seen in the seismic data. Location of the example is shown in Figure 21.*

Structure

The structural complexity of the study area is reflected in the seismic and gravity data (Figure 3). The area is dominated by a series of compartmentalised graben, half-graben and, to a lesser extent (particularly in the south and east), sag basins. Major depocentres commonly correspond to the gravity lows shown in Figure 3. The largest depocentres are located in the north and west of the study area, where they are up to 120 km long and 40 km wide (Figure 12).

Considerable subsidence has occurred across the area, contributing to the present-day water depths of 1200 m in the east to 3000 m in the west. The compartmentalised nature of depocentres and large intervening areas of structural high suggest that there was limited amount of mechanical extension in the upper crust, and that much of the subsidence was driven by lower crustal (ductile) processes. The only reliable deep refraction experiments in the area give a crustal thickness (Moho depth minus the water depth) of about 16.5 km at a site (1597-16) 12 km north of the southern end of line GA-302/16, and 28 km at a site (1597-17) approximately 50 km east of the southern end of line GA-302/12 on the Lord Howe Platform (Shor et al, 1971; Figure 3). In the French (New Caledonian) part of the Lord Howe Rise to the north of the study area, Klingelhoefer et al. (2007) recorded a crustal thickness of 23 km. These crustal thickness values are considerably less than those of typical unthinned continental crust, but crustal velocities in the region are similar to those in eastern Australia (Shor et al, 1971). These results strongly suggest that the Lord Howe Rise is underlain by extended continental crust.

FAULTING

Numerous faults of varying age and type are distributed throughout the study area (see Figures 23 and 25). Two major fault types have been interpreted through the seismic grid: depocentre-bounding faults and large basement-involved intra-basin faults (CF_Flt1); and other major intra-basin faults (CF_Flt2; Table 1) . No attempt has been made to interpret the widely distributed Cenozoic faults with small offsets present in the Upper Sag package of the Post-rift Megasequence (see Figure 20b). Most of these Cenozoic faults are polygonal faults, probably related to sediment dewatering or fluid migration from deeper parts of the depocentres (see Appendix 2).

Most of the depocentre-bounding CF_Flt1 faults offset both the Syn-rift 1 and Syn-rift 2 megasequences (Figures 13, 16, 23 and 25) and terminate at the top of the Syn-rift 2 Megasequence (horizon CF_Sr2B, ?Campanian; Table 1). However, some depocentre-bounding faults extend further upward into the Post-rift Megasequence. Many of the intra-basin CF_Flt1 faults extend from the basement upward into the Syn-rift 1 sediments (Figures 13 and 23). A few intra-basin CF_Flt1 faults extend through to the Syn-rift 2 Megasequence (Figures 16 and 25), but rarely beyond the top of the megasequence (horizon CF_Sr2B; Table 1). Many CF_Flt1 faults in the western parts of the study area (i.e. the western Capel Basin) dip to the west or southwest, whereas many of those in the central and eastern parts dip to the east or northeast (Figures 4, 13 and 16). Moreover, the Syn-rift 2 sediments exhibit significant growth into the westerly-dipping CF_Flt1 faults in the western part of the study area (Figures 4 and 16), while the Syn-rift 1 sediments commonly exhibit growth into both easterly- and westerly-dipping CF_Flt1 faults throughout the study area (Figures 4 and 13).

Many CF_Flt2 intra-basin faults occur entirely within the Syn-rift 1 Megasequence, sometimes occurring as synthetic and antithetic faults to larger CF_Flt1 faults (Figures 13 and 23). In the western parts of the study area, a generation of CF_Flt2 faults occur within the Syn-rift 2 Megasequence (Figures16 and 25) and terminate at the top of the megasequence (horizon CF_Sr2B; Table 1) or, in some cases, extend into the lower Post-Rift Megasequence (up to the horizon CF_Usag; Table 1).

The geometric relationships between major faults and the megasequences indicate a marked westward shift in the locus of faulting and maximum accommodation space generation between Syn-rift 1 and Syn-rift 2 times (Figures 4, 13 and 16). Fault-bounded depocentres were initially formed during the Syn-rift 1 time through movement on the easterly- and westerly-dipping CF_Flt 1 faults. Growth of the Syn-rift 1 sediments into the CF_Flt 1 faults indicates that most of the study area was affected by faulting during this phase. By contrast, during the Syn-rift 2 time, only the western parts of the study area were affected by major movement on westerly-dipping CF_Flt1 faults. Many of these faults were probably initiated during the Syn-rift 1 time. This episode of faulting created significant accommodation for the deposition of Syn-rift 2 Megasequence in the western parts of the study area, and syn-depositional faulting (CF_Flt 2 faults) of the Syn-rift 2 sediments. In the central and eastern areas, smaller movement on existing CF_Flt1 faults created a limited amount of accommodation for the Syn-rift 2 Megasequence.

The temporal change in the location of faulting agrees with the notion that widespread extension during the Syn-rift 1 time in the study area was part of the regionally extensive Early Cretaceous extension along the eastern Gondwana margin (Bryan et al., 1997; Norvick et al., 2008). During the Syn-rift 2 phase, extension became more focused to the west of the study area, supporting the notion that the event was part of the Late Cretaceous extension that eventually led to the opening of the Tasman Sea and the Middleton Basin to the west of the Capel and Faust basins. The progressive focusing of the rift axis was perhaps assisted by crustal weaknesses arising from the Syn-rift 1 extension, or pre-rift structures within the basement such as fault zones, sutures and belts of incompetent lithology.

The numerous faults, structural complexity (including out-of-seismic-plane movements), reactivation and the wide line spacing (generally 15–40 km) make the interpolation of faults between the seismic lines difficult. GOCAD™ software has assisted in this regard by providing a 3D workspace for the integration and interpretation of multiple data sets such as the seismic, gravity, magnetic and multibeam bathymetry, and the modelling of 3D horizon and fault surfaces (see Higgins et al., in prep.). A number of fault trends have been identified through this work; these will be described and interpreted in later publications.

BASIN INVERSION AND FAULT REACTIVATION

Several of the major depocentres shown in Figures 13 and 16 show evidence of a switch from an extensional to probable transpressional deformation, accompanied by uplift and erosion of structural highs, gentle folding of basin sediments, fault reactivation and localised inversion on some faults. These structuring episodes occurred at or after the end of both Syn-rift 1 and Syn-rift 2 depositional phases (Figures 23 and 25). As previously noted, deformation at the end of the Syn-rift 1 phase is probably associated with a regional structuring event in eastern Australia, arising from a major reorganisation of the Australia–Pacific plate boundary (Veevers, 2000; Norvick et al., 2001, 2008; Willcox et al., 2001; Crawford et al., 2003; Schellart et al., 2006; Rey and Müller, 2010). Structuring at the end of the Syn-rift 2 phase was likely to be triggered by the continental breakup associated with the Tasman Sea opening (Norvick et al., 2001, 2008).

Gentle folding and reactivation of syn-rift faults have also affected the Cenozoic sediments, suggesting ongoing episodic structuring during the Post-rift phase. In particular, major structuring events during the Paleocene–Eocene and Eocene–Oligocene resulted in the planation of structural highs and a depositional hiatus within the depocentres, marked by the CF_Eoc and CF_Olig unconformities (Table 1). The Eocene–Oligocene unconformity is observed widely across the Lord Howe Rise and offshore New Zealand regions, e.g. at DSDP holes 206, 207 and 208 (The Shipboard Scientific Party, 1973a, 1973b, 1973c), and has been attributed to a major reorgnisation of plate motion and boundaries in the Pacific (e.g. Veevers, 2000; Crawford et al., 2003; Schellart et al., 2006; Whattam et al., 2008; Sutherland et al., 2010) and regional oceanographic changes (Burns and Andrews, 1973). In some cases (e.g. Figure 27), there is evidence of fault reactivation occurring to the present, resulting in fault scarps and mass movement at the seafloor (Figures 23 and 27, Appendix 2).

It is apparent that individual depocentres within the study area have responded to stress during these structuring events in different ways. The reasons for this spatial variability may include heterogeneities in composition of the basement (for example the "layered", "bland" and "volcanic" types) and basin-fill sediments, structural weaknesses within the basement, and changing regional stress patterns. Several of these possibilities are speculated on by Norvick et al. (2008).

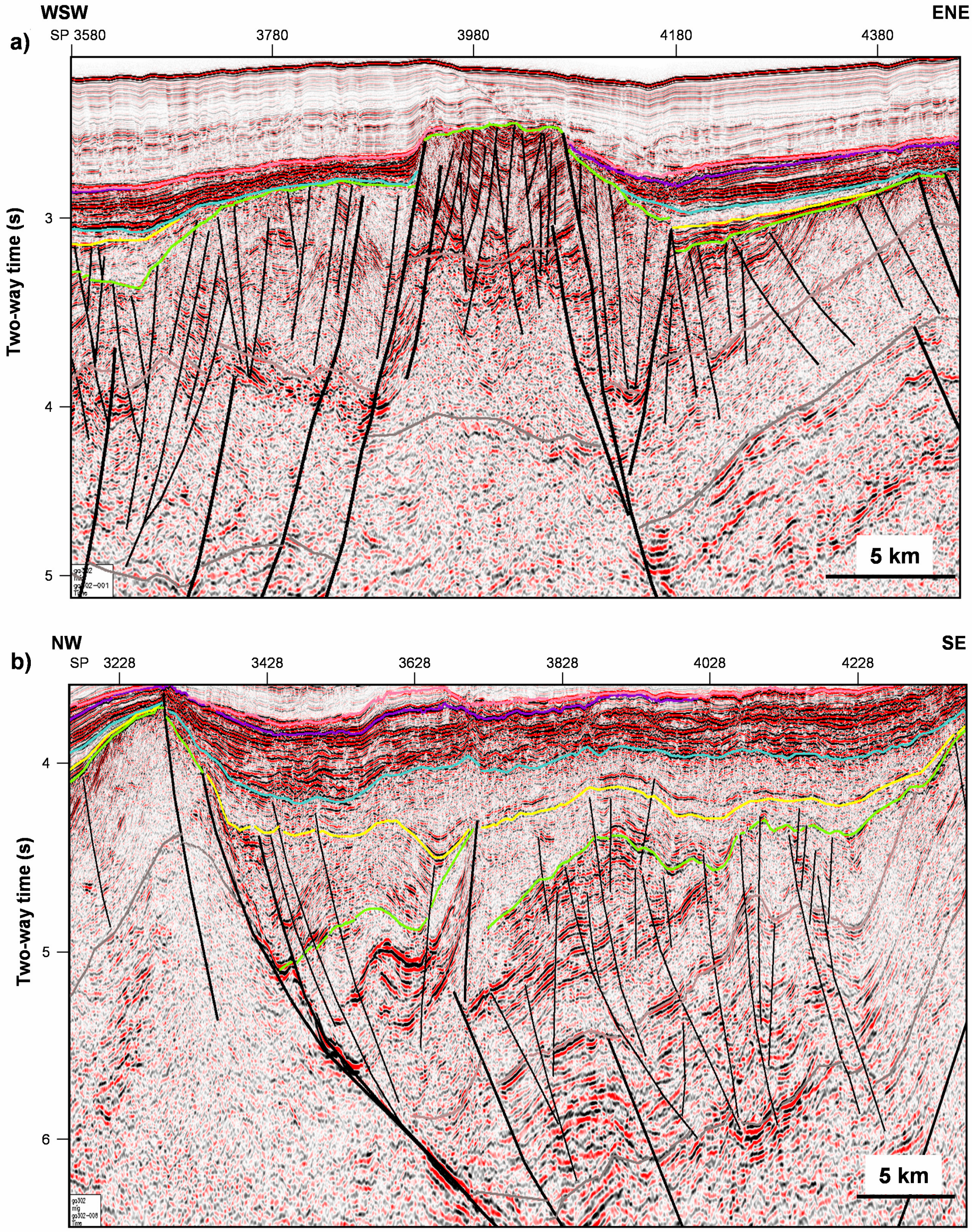

Figure 23: *Examples of structuring within the Syn-rift 1 Megasequence seen in the seismic data. Note the prominent 'pop-up' structure composed of Syn-rift 1 sediments at the centre of (a). See Table 1 for identification of the coloured horizons and Figure 24 for the location of the examples.*

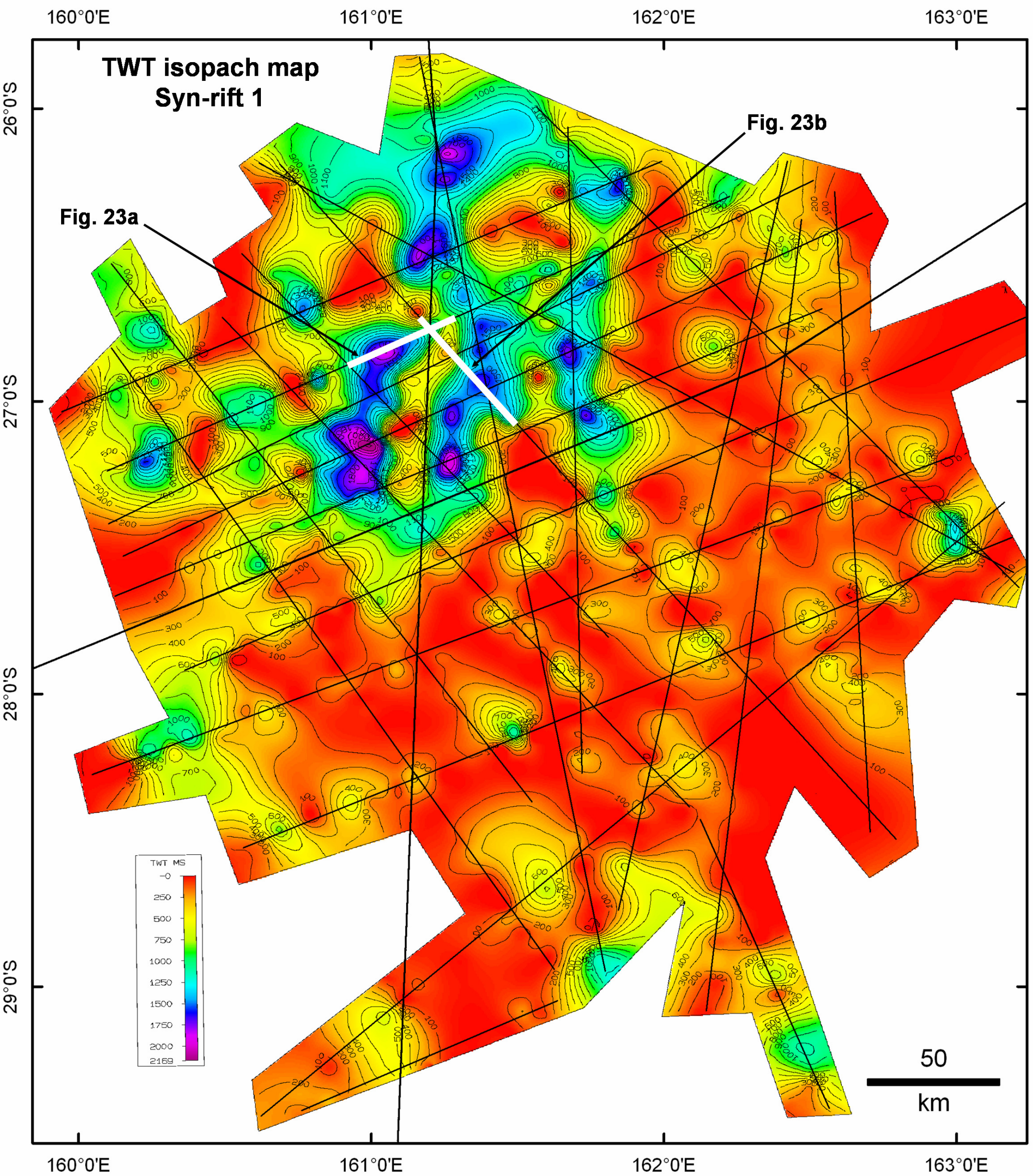

Figure 24: *Location of the examples shown in Figures 23 and 27. Base map is the Syn-Rift 1 time isopach map (Figure 14).*

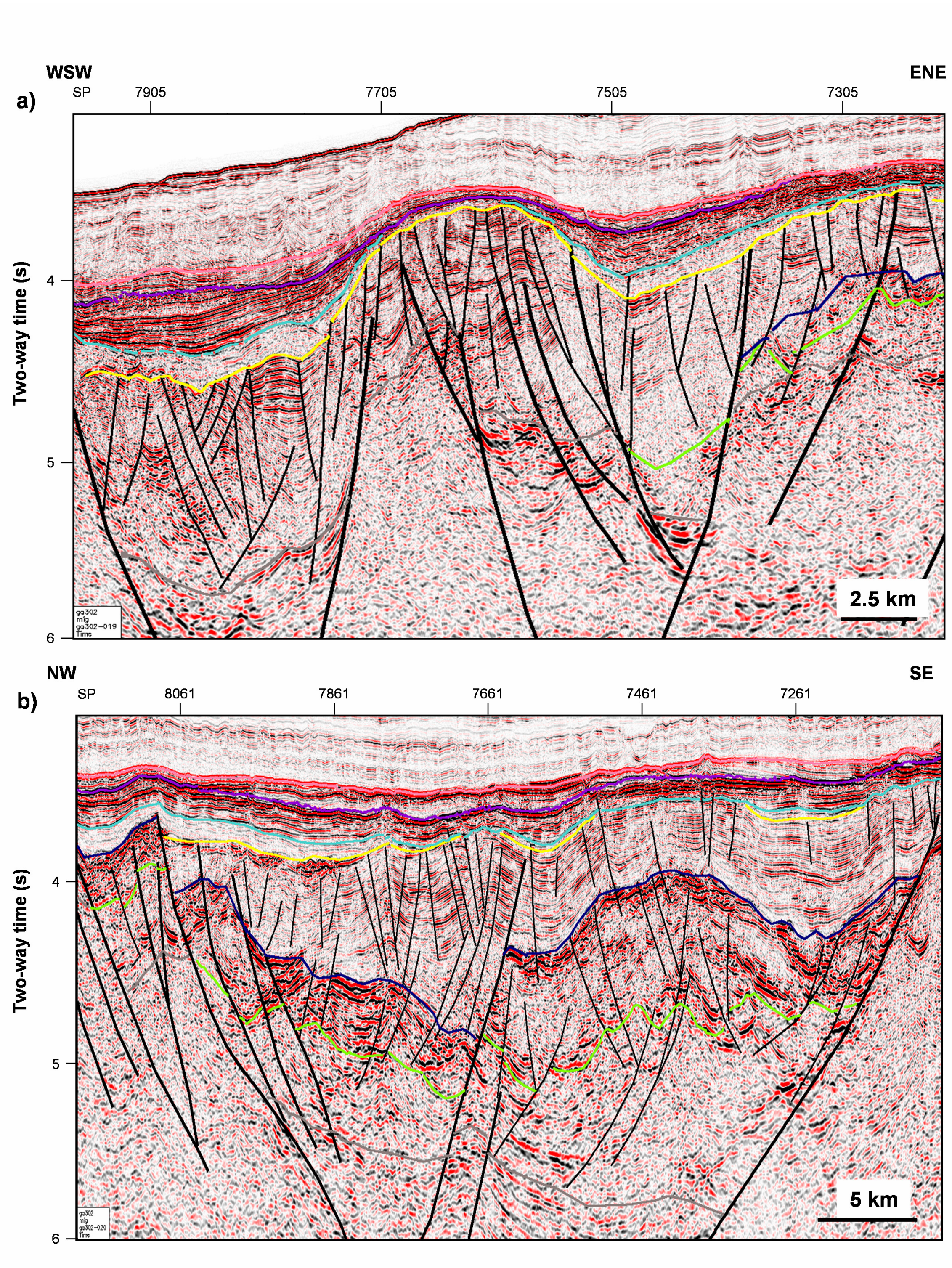

Figure 25: *Examples of the structuring within the Syn-rift 2 Megasequence seen in the seismic data. Note the prominent 'pop-up' structure composed of Syn-rift 2 sediments at the centre of (a) and associated folding and onlap of the overlying Post-rift Megasequence. See Table 1 for identification of the coloured horizons and Figure 26 for the location of the examples.*

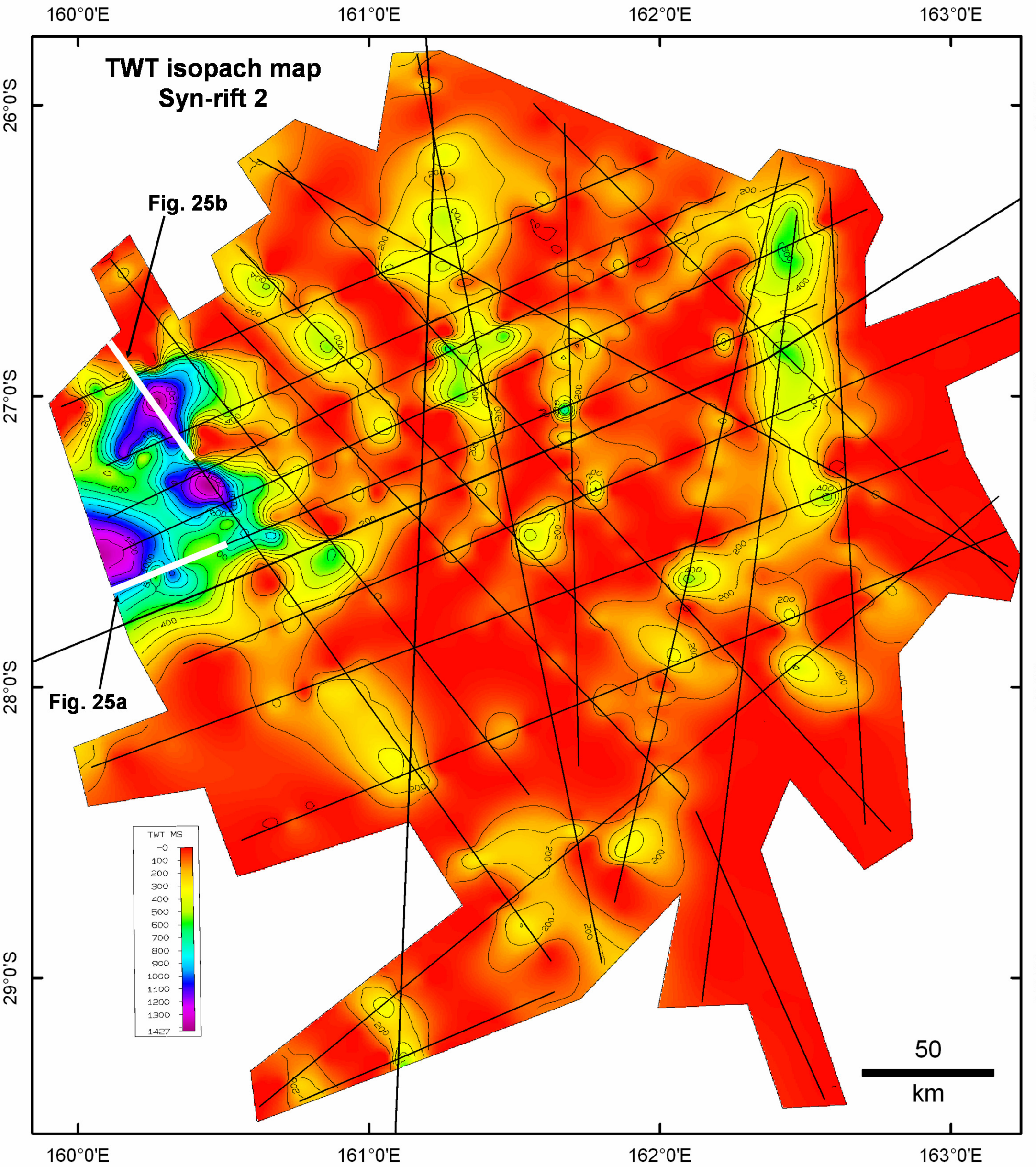

Figure 26: *Location of the examples shown in Figure 25. Base map is the Syn-rift 2 time isopach map (Figure 17).*

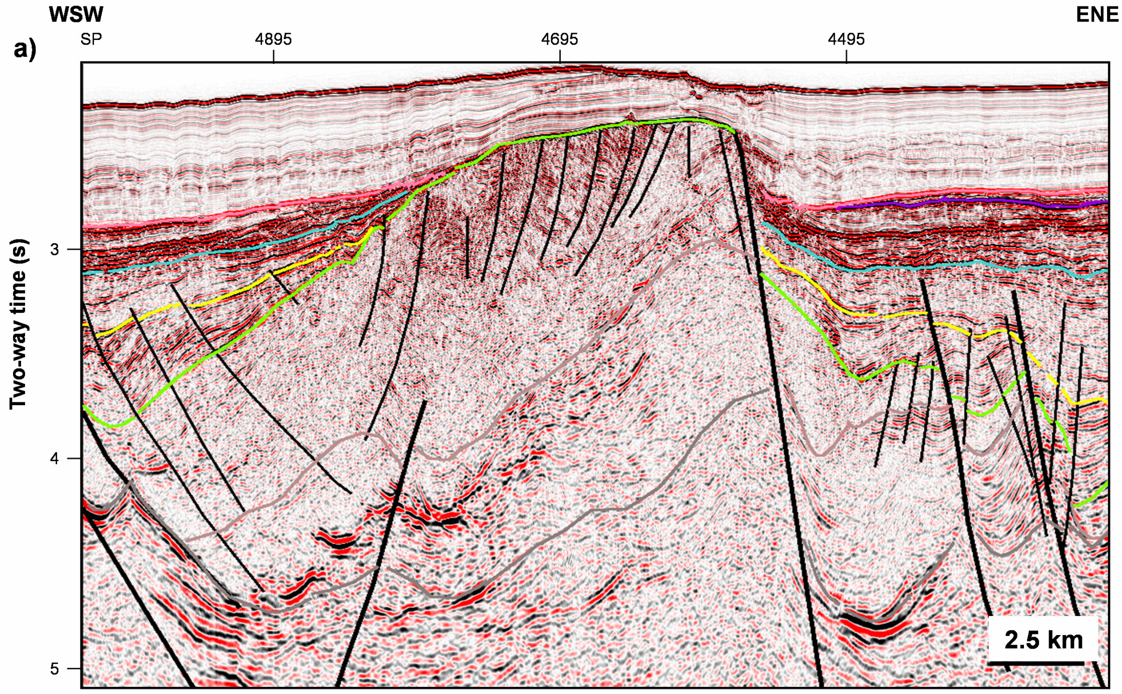

Figure 27: *Example of basin inversion and fault reactivation seen in the seismic data. See Table 1 for identification of the coloured horizons and Figure 28 for the location of the example. Continued movement on the main fault (centre right) has produced a seafloor scarp, followed by current erosion and/or non-deposition on the face of the scarp. These types of seafloor features are well imaged on the GA survey 2436 (TAN031) swath bathymetry data (see Heap et al., 2009).*

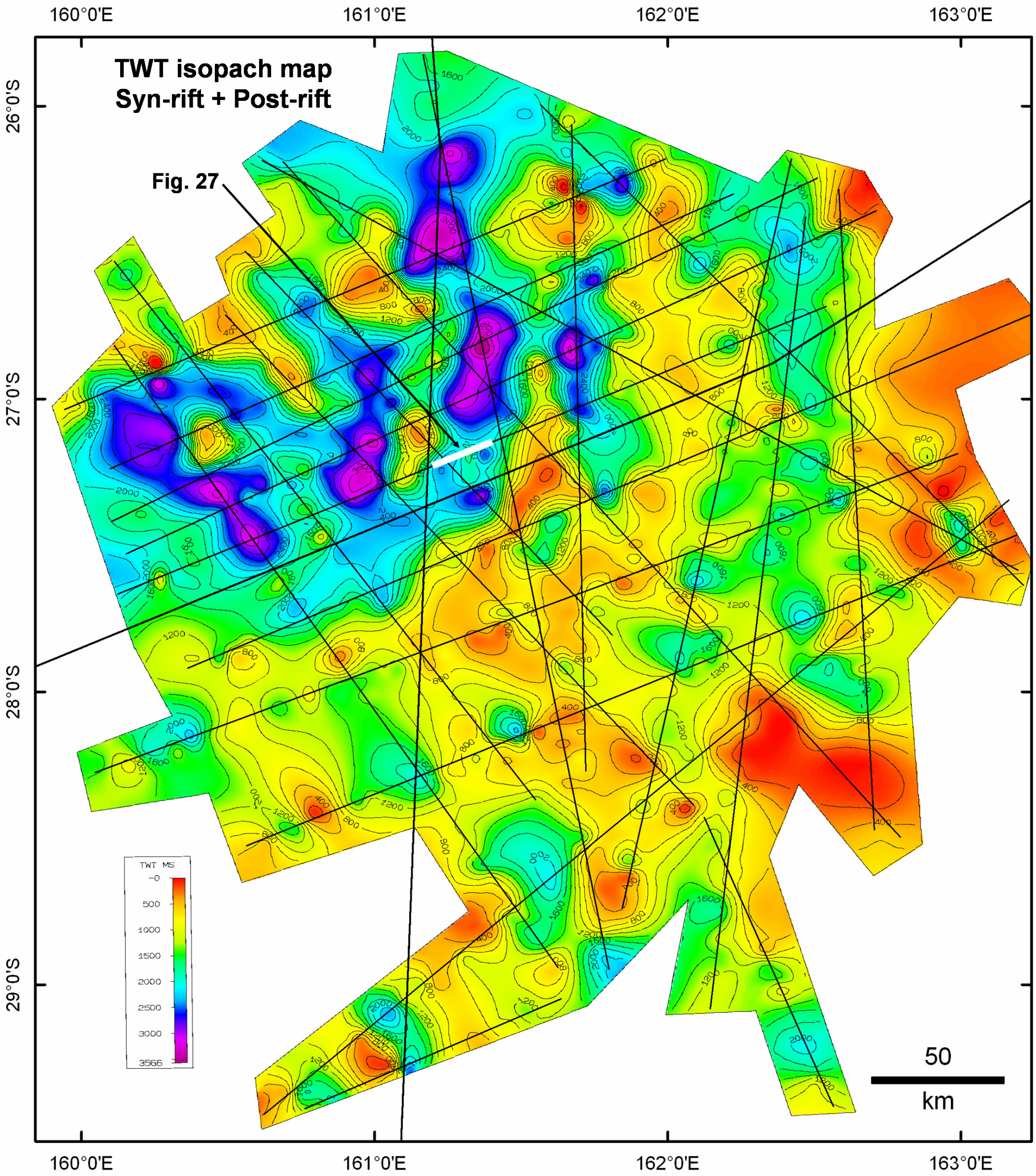

Figure 28: *Location of the example shown in Figure 27. Base map is the total sediment thickness above basement in milliseconds TWT (Figure 12).*

Conclusions and Future Directions

The seismic interpretation presented in this record forms part of the ongoing geological and petroleum prospectivity assessment of the Capel and Faust basins by GA's Remote Eastern Frontiers Project (Hashimoto et al., 2009, 2010). A key aspect of this evaluation involves the integration of the interpreted seismic data (this record) with potential field data (Hackney, 2010) and potential field modelling (Petkovic, 2010; Petkovic et al., in press) in a 3D environment (Higgins et al., in prep.).

The seismic data has revealed the existence of major fault-bounded depocentres in the northwestern and central parts of the seismic grid, where the total syn-rift to post-rift sediment thickness reaches 3.6 seconds TWT. Two Cretaceous syn-rift and one Upper Cretaceous to Cenozoic post-rift seismic megasequences have been identified. The syn-rift megasequences appear to contain a substantial igneous and volcaniclastic component, as well as coaly intervals that may provide potential source rocks. The Syn-rift 2 to lower Post-rift megasequences may potentially contain reservoir-quality fluvio-deltaic and marine sandstones. Fine-grained bathyal sediments in the Post-rift Megasequence may provide a regional seal. The underlying pre-rift basement appears to be heterogeneous in composition and, in places may include an older sedimentary succession. These pre-rift sediments are probably the correlatives of coal-bearing Mesozoic successions in eastern Australia and, thus, may have source rock potential.

The study area is structurally complex, comprising multiple compartmentalised graben and half-graben separated by structural highs. Transpressional(?) structuring events affected the area at or after the end of each syn-rift phase and during the Cenozoic, resulting in local fault reactivation, basin inversion, uplift, erosion and gentle folding. Minor deformation has continued to the present, affecting the seafloor geomorphology. Some of the structures may provide potential traps for hydrocarbons, but the timing of trap formation requires assessment against the history of burial and hydrocarbon generation. Multiple unconformities and the lateral and vertical lithological heterogeneity within the syn-rift and post-rift megasequences suggest considerable potential for stratigraphic traps.

Ongoing work in the project will improve the understanding of the basins' regional tectonostratigraphic context, and of their petroleum generation and trapping potential through geohistory modelling. The results of preliminary 1D geohistory modelling suggest that the deeper parts of the basins reach the oil and gas windows (Hashimoto et al., 2009, 2010).

The greatest limitation to the understanding of the basins' petroleum prospectivity comes from the lack of age and lithological control over most of the sedimentary succession, which could be resolved through future stratigraphic drilling. In the meantime, the inferences will have to rely largely on analogue studies of better-constrained basins in the region, e.g. the Taranaki and Northland basins of New Zealand.

Although 3D data integration and visualisation applied within the project has improved the confidence of data interpolation between the seismic lines, the relatively wide line spacing results in a significant degree of uncertainty regarding the 3D structure of the study area. To this end, the results of the current seismic interpretation could be used, in conjunction with gravity data, to identify targets and to guide the line placement for a future high-density 2D or 3D seismic survey. At the regional scale, future acquisition of deep-crustal seismic reflection and refraction data would provide further insights into the large-scale structural and evolutionary context of the Capel and Faust basins within the Cretaceous eastern Gondwanan rift system.

References

Andrews, J. E., 1973. Correlation of seismic reflectors. *In:* Burns R. E., Andrews, J. E. et al. (Eds.), *Initial Reports of the Deep Sea Drilling Project,* **21**, US Government Printing Office, Washington, 459–479.

Auzende, J-M., Beneton, G., Dickens, G., Exon, N., François, C., Hodway, D., Juffroy, F., Lafoy, Y., Leroy, A., van de Beuque, S. and Voutay, O., 2000a. Mise en évidence de diapirs mésozoïques sur la bordure orientale de la ride de Lord Howe (sud-ouest Pacifique): campagne ZoNéCo 5. *Comptes Rendus de l'Académie de Science Paris, Sciences de la Terre et des Planètes*, **330**, 209–215.

Auzende, J-M., Dickens, G. R., van de Beuque, S., Exon, N. F., François, C., Lafoy, Y. and Voutay, O., 2000b. Thinned crust in southwest Pacific may harbor gas hydrate. *EOS,* **81**, 182–185.

Auzende, J-M., van de Beuque, S., Dickens, G., François, C., Lafoy, Y., Voutay, O. and Exon, N., 2000c. Deep sea diapirs and bottom simulating reflector in Fairway Basin (SW Pacific). *Marine Geophysical Researches,* **21**, 579–587.

Bernardel, G., Lafoy, Y., van de Beuque, S., Missegue, F. and Nercessian, A., 1999. Preliminary results from AGSO Law of the Sea Cruise 206: an Australian/French collaborative deep-seismic marine survey in the Lord Howe Rise/New Caledonia region. *Australian Geological Survey Organisation Record,* **1999/14**.

Bernecker, T. and Partridge, A. D., 2001. Emperor and Golden Beach Sub-groups: the onset of Late Cretaceous sedimentation in the Gippsland Basin. *In*: Hill, K. C. and Bernecker, T., (Eds.), Eastern Australasian Basins Symposium; a refocused energy perspective for the future, *Petroleum Exploration Society of Australia Special Publication*, 391–402.

Bernecker, T., Woollands, M. A., Wong, D., Moore, D. H. and Smith, M. A., 2001. Hydrocarbon prospectivity of the deep water Gippsland Basin, Victoria, Australia. *APPEA Journal*, **41**(1), 91–113.

Blevin, J.E., Trigg, K. R., Partridge, A. D., Boreham, C. J. and Lang, S. C., 2005. Tectonostratigraphy and potential source rocks of the Bass Basin. *APPEA Journal*, **45**(1), 601–621.

Bryan, S. E., Constantine, A. E., Stephens, C. J., Ewart, A., Schon, R. W. and Parianos, J., 1997. Early Cretaceous volcano-sedimentary successions along the eastern Australian continental margin: implications for the breakup of eastern Gondwana. *Earth and Planetary Science Letters*, **153**, 85–102.

Bryan, S. E., Ewart, A., Stephens, C. J., Parianos, J. and Downes, P. J., 2000. The Whitsunday volcanic province, central Queensland, Australia: lithological and stratigraphic investigations of a silicic-dominated large igneous province. *Journal of Volcanology and Geothermal Research*, **99**, 55–78.

Colwell, J., Foucher, J-P., Logan, G. and Balut, Y., 2006. Partie 2, Programme AUSFAIR (Australia–Fairway basin bathymetry and sampling survey) Cruise Report. *In: Les rapports de campagnes à la mer, MD 153/AUSFAIR–ZoNéCo 12 and VT 82/GAB on board R/V Marion Dufresne*, Institut Polaire Français Paul Emile Victor, Plouzané, France, Réf : OCE/2006/05.

Cook, R. A., Sutherland, R. and Zhu, H., 1999. Cretaceous–Cenozoic geology and petroleum systems of the Great South Basin, New Zealand. *Institute of Geological and Nuclear Sciences Mononograph*, **21**.

Crawford, A. J., Mèffre, S. and Symonds, P. A., 2003. 120 to 0 Ma tectonic evolution of the southwest Pacific and analogous geological evolution of the 600 to 220 Ma Tasman Fold Belt System. *In:* Hillis, R. R. and Müller, R. D. (Eds.), Evolution and dynamics of the Australian Plate, *Geological Society of Australia Special Publication*, **22** and *Geological Society of America Special Publication*, **372**, 383–403.

Ellis, P. L., 1968. Geology of the Maryborough 1:250,000 sheet area. *Geological Survey of Queensland Report*, **26**.

Etheridge, M. A., Symonds, P. A. and Lister, G. S., 1989. Application of the detachment model to reconstruction of conjugate passive margins. *In*: Tankard, A. J. and Balkwill, H. R. (Eds.), Extensional tectonics and stratigraphy of the North Atlantic margins, *American Association of Petroleum Geologists Memoir*, **46**, 23–40.

Exon, N. F., Dickens, G. R., Auzende, J-M., Lafoy, Y., Symonds, P. A. and van de Beuque, S., 1998. Gas hydrates and free gas on the Lord Howe Rise. *Petroleum Exploration Society of Australia Journal*, **26**, 148–58.

Exon, N., Hill, P., Lafoy, Y., Fellows, M., Perry, K., Mitts, P., Howe, R., Chaproniere, G., Dickens, G., Ussler, W. and Paull, C., 2004. Geology of the Fairway and New Caledonia Basins in the Tasman Sea: sediment, pore water, diapirs and bottom simulating reflectors (Franklin Cruise FR9/01 and Geoscience Australia Survey 232). *Geoscience Australia Record*, **2004/26**.

Exon, N. F., Quilty, P. G., Lafoy, Y., Crawford, A. J. and Auzende, J-M., 2004. Miocene volcanic seamounts on northern Lord Howe Rise: lithology, age and origin. *Australian Journal of Earth Sciences*, **51**(2), 291–300.

Exon, N. F., Lafoy, Y., Hill, P. J., Dickens, G. R. and Pecher, I., 2007. Geology and petroleum potential of the Fairway Basin in the Tasman Sea. *Australian Journal of Earth Sciences*, **54**(5), 629–645.

Gaina, C., Müller, D. R., Royer, J-Y., Stock, J., Hardebeck, J. and Symonds, P., 1998. The tectonic history of the Tasman Sea: a puzzle with 13 pieces. *Journal of Geophysical Research*, **103**(B6), 12413–12433.

Hackney, R., 2010. Potential-field data covering the Capel and Faust Basins, Australia's Remote Offshore Eastern Frontier. *Geoscience Australia Record*, **2010/34**.

Hackney, R., Hashimoto, R., Higgins, K., Petkovic, P., Rollet, N., Logan, G., Colwell, J. and Morse, M., 2009a. Australia's eastern margin: geophysical studies of remote deep-water frontier basins. *Abstracts 69th Annual Meeting of the German Geophysical Society*, 93.

Hackney, R., Petkovic, P., Hashimoto, T., Higgins, K., Logan, G., Bernardel, G., Colwell, J., Rollet, N. and Morse, M., 2009b. Geophysical studies of Australia's remote eastern deep-water frontier: results from the Capel and Faust Basins. *Australian Society of Exploration Geophysicists Extended Abstracts*, **2009**(1).

Hackney, R., Morse, M. and Johnston, S. 2010. Challenges in the use of potential field data for studies of remote deep-water frontier basins. 21st International Geophysical Conference and Exhibition, *Australian Society of Exploration Geophysicists and Petroleum Exploration Society of Australia Extended Abstracts*, **2010**(1).

Hashimoto, T., Langford, R., Rollet, N., Earl, K. and Bernardel, G., 2008a. Capel and Faust basins—geoscientific assessment of an offshore frontier region. *In:* Australian Earth Sciences Convention (AESC) 2008 and 19th Australian Geological Convention, Program and Abstract Booklet, *Geological Society of Australia* and *the Australian Institute of Geoscientists Abstracts*, **89**, 128.

Hashimoto, T., Rollet, N., Earl, K. and Bernardel, G., 2008b. Capel and Faust basins—new information from the offshore frontier between Australia, New Zealand and New Caledonia. *2008 New Zealand Petroleum Conference Proceedings*.

Hashimoto, T., Rollet, N., Higgins, K., Bernardel, G. and Hackney, R. 2008c. Capel and Faust basins: Preliminary assessment of an offshore deepwater frontier region. *In*: Blevin, J. E., Bradshaw, B. E. and Uruski, C. (Eds), Eastern Australasian Basins Symposium III: Energy security for the 21st century, *Petroleum Exploration Society of Australia Special Publication*, 311–316.

Hashimoto, T., Higgins, K., Hackney, R. Stagpoole, V., Uruski, C., Rollet, N., Bernardel, G., Logan, G. and Sutherland, R., 2009. Capel and Faust basins—integrated geoscientific assessment of Australia's remote offshore eastern frontier. The Australian Petroleum Production and Exploration Association Conference 2009 Extended Abstracts. *The APPEA Journal*, **49**.

Hashimoto, T., Higgins, K., Stagpoole, V., Rollet, N., Petkovic, P., Hackney, R., Bernardel, G. and Colwell, J., 2010. Geology of the Capel and Faust basins— implications for prospectivity of remote deepwater frontier basins of the Tasman Sea. *2010 New Zealand Petroleum Conference Proceedings*.

Hayes, D. E. and Ringis, J., 1973. Seafloor spreading in the Tasman Sea. *Nature*, **243**, 454–458.

Heap, A. D., Hughes, M., Anderson, T., Nichol, S., Hashimoto, T., Daniell, J., Przeslawski, R., Payne, D., Radke, L. and Shipboard Party, 2009. Seabed environments of the Capel and Faust basins and Gifford Guyot, eastern Australia, TAN0713 post-survey report. *Geoscience Australia Record*, **2009/22**.

Herzer, R. H., Chaproniere, G. C. H., Edwards, A. R., Hollis, C. J., Pelletier, B., Raine, J. I., Scott,G. H., Stagpoole, V., Strong, C. P., Symonds, P., Wilson, G. J. and Zhu, H., 1997. Seismic stratigraphy and structural history of the Reinga Basin and its margins, southern Norfolk Ridge system. *New Zealand Journal of Geology and Geophysics*, **40**, 425–451.

Herzer, R. H., Sykes, R., Killops, S. D., Funnell, R. H., Burggraf, D. R., Townend, J., Raine, J. I. and Wilson, G. J., 1999. Cretaceous carbonaceous rocks from the Norfolk Ridge system, Southwest Pacific: implications for regional petroleum potential. *New Zealand Journal of Geology and Geophysics*, **42**, 57–73.

Higgins, K. L., Hashimoto, T., Hackney, T., Petkovic, P. and Milligan, P., in prep. 3D Geological Modelling and Petroleum Prospectivity Assessment in Offshore Frontier Basins using GOCAD^{TM}: Capel and Faust Basins, Lord Howe Rise. *Geoscience Australia Record*.

Higgins, K., Hashimoto, T., Fraser, G., Rollet, N. and Colwell, J., in press. Ion microprobe (SHRIMP) U-Pb dating of Upper Cretaceous volcanics from the northern Lord Howe Rise, Tasman Sea. *Australian Journal of Earth Sciences*.

Hill, P. J., 1994. Geology and geophysics of the offshore Maryborough, Capricorn and northern Tasman Basins: results of AGSO Survey 91. *Australian Geological Survey Organisation Record*, **1994/1**.

Jongsma, D. and Mutter, J. C., 1978. Non-axial breaching of a rift valley: evidence from the Lord Howe Rise and the southeastern Australian margin. *Earth and Planetary Science Letters*, **39**, 226–234.

Killops, S. D., Cook, R. A., Sykes, R. and Boudou, J. P., 1997. Petroleum potential and oil-source correlation in the Great South and Canterbury Basins. *New Zealand Journal of Geology and Geophysics*, **40**, 405–423.

King, P. R. and Thrasher, G. P., 1996. Cretaceous–Cenozoic geology and petroleum systems of the Taranaki Basin, New Zealand. *Institute of Geological and Nuclear Sciences Monograph*, **13**.

Klingelhoefer, F., Lafoy, Y., Collot, J., Cosquer, E., Géli, L., Nouzé, H. and Vially, R., 2007. Crustal structure of the basin and ridge system west of New Caledonia (southwest Pacific) from wide-angle and reflection seismic data. *Journal of Geophysical Research*, **112**(B11102), doi:10.1029/2007JB005093.

Krassay, A. A., Cathro, D. L. and Ryan, D. J., 2004. A regional tectonostratigraphic framework for the Otway Basin. *In:* Boult, P. J., Johns, D. R. and Lang, S. C., (Eds.), Eastern Australasian Basins Symposium II, *Petroleum Exploration Society of Australia Special Publication*, 97–116.

Kroh, F., Morse, M. P. and Hashimoto, T., 2007. New data on the Capel and Faust basins. *Preview*, **130**, 22–24.

Lafoy, Y., van de Beuque, S., Bernardel, G., Missegue, F., Nercessian A., Auzende, J-M., Symonds, P. and Exon, N., 1998a. Scientists study deep geological structure between New Hebrides arc and eastern Australian margin. *EOS*, **79**, 613–614.

Lafoy, Y., van de Beuque, S., Missegue, F., Nercessian, A. and Bernardel, G., 1998b. Campagne de sismique multitraces entre la marge est Australienne et le sud de l'arc des Nouvelles-Hébrides: rapport de la campagne Rig Seismic 206 (21 avril–24 mai 1998). *Programme FAUST (French–Australian Seismic Transect) Rapport ZoNéCo*.

Lafoy, Y., Brodien, I., Vially, R. and Exon, N. F., 2005. Structure of the basin and ridge system west of New Caledonia (Southwest Pacific); a synthesis. *Marine Geophysical Researches*, **26**, 37–50.

McDougall I. and van der Lingen G. J., 1974. Age of the rhyolites of the Lord Howe Rise and the evolution of the southwest Pacific Ocean. *Earth and Planetary Science Letters*, **21**, 117–126.

McDougall, I., Embleton, B. J. J. and Stone, D. B., 1981. Origin and evolution of Lord Howe Island, Southwest Pacific. *Journal of the Geological Society of Australia*, **28**, 155–176.

McDougall, I., Maboko, M. A. H., Symonds, P. A., McCulloch, M. T., Williams, I. S. and Kudrass, H. R., 1994. Dampier Ridge, Tasman Sea, as a stranded continental fragment. *Australian Journal of Earth Sciences*, **41**(5) 395–406.

Mortimer, N., Herzer, R. H., Gans, P. B., Parkinson, D. L. and Seward, D., 1998. Basement geology from Three Kings Ridge to West Norfolk Ridge, southwest Pacific Ocean: evidence from petrology, geochemistry and isotope dating of dredge samples. *Marine Geology*, **148**, 135–162.

Mortimer, N., Hauff, F. and Calvert, T., 2008. Continuation of the New England Orogen, Australia, beneath the Queensland Plateau and Lord Howe Rise. *Australian Journal of Earth Sciences*, **55**, 195–209.

Norvick, M. S., Langford, R. P., Rollet, N., Hashimoto, T., Earl, K. L. and Morse, M. P., 2008. New insights into the evolution of the Lord Howe Rise (Capel and Faust basins), offshore eastern Australia, from terrane and geophysical data analysis. *In*: Blevin, J. E., Bradshaw, B. E. and Uruski, C. (Eds.), Eastern Australasian Basins Symposium III: Energy security for the 21st century, *Petroleum Exploration Society of Australia Special Publication*, 291–310.

Norvick, M. S., Smith, M. A. and Power, M. R., 2001. The plate tectonic evolution of eastern Australasia guided by the stratigraphy of the Gippsland Basin. *In*: Hill, K. C. and Bernecker, T. (Eds.), Eastern Australasian Basins Symposium: a refocussed energy perspective for the future, *Petroleum Exploration Society of Australia Special Publication,* 15–24.

Nouzé, H., Lafoy, Y., Géli, L., Klingelhoefer, F. and Shipboard Party, 2005. First results of a high resolution seismic study of a Bottom Simulating Reflector in the Fairway Basin, offshore New Caledonia. *Fifth International Conference on Gas Hydrates (ICGH 5), Trondheim, Norway*.

Nouzé, H., Cosquer, E., Collot, J., Foucher, J-P., Klingelhoefer, F., Lafoy, Y. and Géli, L., 2009. Geophysical characterisation of bottom simulating reflectors in the Fairway Basin (off New Caledonia, Southwest Pacific), based on high resolution seismic profiles and heat flow data. *Marine Geology*, **266**, 80–90.

Petkovic, P., Hackney, R., Hashimoto, T., Higgins, K., Logan, G. and Rollet, N., 2008. Gravity constraints on the architecture of the Capel and Faust basins, northern Tasman Sea, *Geological Society of New Zealand Miscellaneous Publication*, **124A**, 113.

Petkovic, P., 2010. Seismic velocity models of the sediment and upper crust of the Capel and Faust Basins, Lord Howe Rise. *Geoscience Australia Record*, **2010/03**.

Petkovic, P., Lane, R., Rollet, N. and Nayak, G. K., 2010. 3D mapping and gravity modelling of Capel and Faust basins. 21st International Geophysical Conference and Exhibition, *Australian Society of Exploration Geophysicists and Petroleum Exploration Society of Australia Extended Abstracts*, **2010**(1).

Ramsay, D. C., Herzer, R. H. and Barnes, P. M., 1997. Continental shelf definition in the Lord Howe Rise and Norfolk Ridge regions: Law of the Sea Survey 177, Part 1—preliminary results. *Australian Geological Survey Organisation Record*, **1997/54**.

Raza, A., Hill, K. C. and Korsch, R. J., 2009. Mid-Cretaceous uplift and denudation of the Bowen and Surat Basins, eastern Australia: relationship to Tasman Sea rifting from apatite fission-track and vitrinite-reflectance data. *Australian Journal of Earth Sciences*, **56**, 501–531.

Rey, P. F. and Müller, R. D., 2010. Fragmentation of active continental plate margins owing to the buoyancy of the mantle wedge. *Nature Geoscience*, NGEO825, DOI:10.1038.

Roeser, H. and Shipboard Party, 1985. Geophysical, geological and geochemical studies on Lord Howe Rise. *Bundesanstalt für Geowissenschaften und Rohstoffe Report*, Cruise SO36(1).

Sandwell, D. T. and Smith, W. H. F., 1997. Marine gravity from Geosat and ERS 1 altimetry. *Journal of Geophysical Research*, **102**(B5), 10039–10054.

Schellart, W. P., Lister, G. S. and Toy, V. G., 2006. A Late Cretaceous and Cenozoic reconstruction of the Southwest Pacific region: tectonics controlled by subduction and slab rollback processes. *Earth-Science Reviews*, **76**, 191–233.

Sdrolias, M., Müller, D. and Gaina, C., 2001. Plate tectonic evolution of eastern Australian marginal ocean basins. *In*: Hill, K. C. and Bernecker, T. (Eds.), Eastern Australasian Basins Symposium: a refocussed energy perspective for the future, *Petroleum Exploration Society of Australia Special Publication,* 227–237.

Shor, G. G., Kirk, H. K. and Menard, H. W., 1971. Crustal Structure of the Melanesian Area. *Journal of Geophysical Research*, **76**(11), 2562–2586.

Slater, R. A. and Goodwin, R. H., 1973. Tasman Sea guyots. *Marine Geology*, **14**, 81–99.

Stagg, H. M. J., Alcock, M. B., Borissova, I. and Moore, A. M. G., 2002. Geological framework of the southern Lord Howe Rise and adjacent areas. *Geoscience Australia Record*, **2002/25**.

Stagg, H. M. J., Borissova, I., Alcock, M. and Moore, A. M. G., 1999. Tectonic provinces of the Lord Howe Rise: Law of the Sea study has implications for frontier hydrocarbons. *AGSO Research Newsletter*, **31**, 31–32.

Stagpoole, V. M., Reid, E., Browne, G. H., Bland, K., Ilg, B., Griffin, A., Herzer, R. H. and Uruski, C. 2009. Petroleum Prospectivity of the Reinga Basin, New Zealand, *GNS Science Consultancy Report*, **2009/251**.

Stephenson, A. E. and Burch, G. J., 2004. Preliminary evaluation of the petroleum potential of Australia's central eastern margin. *Geoscience Australia Record*, **2004/06**.

Sutherland, R., Collot, J., Lafoy, Y., Logan, G. A., Hackney, R., Stagpoole, V., Uruski, C., Hashimoto, T., Higgins, K., Herzer, R. H., Wood, R., Mortimer, N. and Rollet, N., 2010. Lithosphere delamination with foundering of lower crust and mantle caused permanent subsidence of New Caledonia Trough and transient uplift of Lord Howe Rise during Eocene and Oligocene initiation of Tonga–Kermadec subduction, western Pacific. *Tectonics*, **29**, TC2004, doi:10.1029/2009TC002476.

The Shipboard Scientific Party, 1973a. Site 206. *In:* Burns, R. E., Andrews, J. E. et al. (Eds.), *Initial Reports of the Deep Sea Drilling Project*, **21**, US Government Printing Office, Washington, 103–195.

The Shipboard Scientific Party, 1973b. Site 207. *In:* Burns, R. E., Andrews, J. E. et al. (Eds.), *Initial Reports of the Deep Sea Drilling Project*, **21**, US Government Printing Office, Washington, 197–269.

The Shipboard Scientific Party, 1973c. Site 208. *In:* Burns, R. E., Andrews, J. E. et al. (Eds.), *Initial Reports of the Deep Sea Drilling Project*, **21**, US Government Printing Office, Washington, 271–331.

Uruski, C. and Baillie, P., 2001. Petroleum potential of New Zealand's deepwater basins. *In:* Hill, K. C., and Bernecker, T., Eastern Australasian Basins Symposium; a refocussed energy perspective for the future, *Petroleum Exploration Society of Australia Special Publication*, 151–158.

Uruski, C. and Baillie, P., 2004. Mesozoic evolution of the greater Taranaki Basin and implications for prospectivity. *APPEA Journal*, **44**, 385–396.

Uruski, C. I., Browne, G. H., Stagpoole, V., Herzer, R. H., Bland, K. J., Griffin, A. G., Sykes, R., Roncaglia, L., Schioler, P., Funnell, R. H., Strong, C. P. and Isaac, M. J. 2008. Petroleum Prospectivity of the Northland Basin, New Zealand. *GNS Science Consultancy Report*, **2008/190**.

Van de Beuque, S., Stagg, H. M. J., Sayers, J., Willcox, J. B. and Symonds, P. A., 2003. Geological framework of the northern Lord Howe Rise and adjacent areas. *Geoscience Australia Record*, **2003/01**.

Veevers, J. J., 2000. Change of tectono-stratigraphic regime in the Australian plate during the 99 Ma (mid-Cretaceous) and 43 ma (mid-Eocene) swerves of the Pacific. *Geology*, **28**(1), 47–50.

Whattam, S. A., Malpas, J., Ali, J. R. and Smith, I. E. M., 2008. New SW Pacific tectonic model: Cyclical intraoceanic magmatic arc construction and near-coeval emplacement along the Australia–Pacific margin in the Cenozoic. Geochemistry Geophysics Geosystems, **9**(3), Q03021, doi:10.1029/2007GC001710

Willcox, J. B. and Sayers, J., 2002. Geological framework of the central Lord Howe Rise (Gower Basin) region. *Geoscience Australia Record*, **2002/11**.

Willcox, J. B., Sayers, J., Stagg, H. M. J. and van de Beuque, S., 2001. Geological framework of the Lord Howe Rise and adjacent oceanic basins. *In*: Hill, K. C. and Bernecker, T. (Eds.), Eastern Australasian Basins Symposium: a refocussed energy perspective for the future, *Petroleum Exploration Society of Australia Special Publication,* 211–225.

Zhu, H. and Symonds, P. A., 1994. Seismic interpretation, gravity modelling and petroleum potential of the southern Lord Howe Rise region. *1994 New Zealand Petroleum Conference Proceedings*, 223–230.